Journal of Applied Mathematics, Statistics, and Computational Sciences
JAMSCS

OA
OPEN ACCESS

Copyright © Authors, 2026

Research Article

Predator–Prey Dynamics from Growth Cycles to Financial Instability: Deterministic Structure and Stochastic Fragility

Deepak Bastola[1,*], Pitambar Acharya[2], Dipak Dulal[3], and Pawan Kumar BK[4]

Received: 2026-07-04
Revised: 2026-08-12
Accepted: 2026-09-09
Published: 2026-10-21

Article:

Open access under the Creative Commons Attribution (CC BY 4.0) license.

[1]Department of Mathematics and Statistics, Florida Atlantic University, FL, USA
[2]Department of Applied Mathematics, University of Alabama at Birmingham, AL, USA
[3]Department of Mathematical Sciences, Eastern New Mexico University, NM, USA
[4]Trichandra Multiple Campus, Tribhuvan University, Kathmandu, Nepal
[*]Corresponding author: dbastola2022@fau.edu
ORCID iDs: Deepak Bastola: 0009-0006-4049-4772; Pitambar Acharya: 0009-0009-5869-2955; Dipak Dulal: 0000-0001-7300-8060

Abstract

This article develops a rigorous, self-contained framework applying predator–prey dynamics to economic and financial systems. Starting from the classical Lotka–Volterra equations with positive invariance, a conserved Hamiltonian, and center-type stability, we derive three socioeconomic models. First, the Goodwin growth-cycle model is exactly algebraically isomorphic to Lotka–Volterra, so endogenous business cycles appear as closed periodic orbits. Second, a two-species debt–capital model formalizes Minsky's Financial Instability Hypothesis: the deterministic system is a neutrally stable center for all positive parameters, while under Itô noise the conserved "energy" drifts outward at rate $\frac{1}{2}(\sigma_C^2 r_D + \sigma_D^2 r_C) > 0$; the ratio r_C/r_D sets equilibrium leverage rather than a stability threshold. Third, in a three-species super-predator extension, the unique interior equilibrium is proved unstable for all positive parameters, and a closed-form transversal exponent decides whether debt is driven to extinction on the boundary. Finally, for a finite-size stochastic buyer–seller market model with herding, we prove convergence in probability, uniformly on compact intervals, to the deterministic Lotka–Volterra ODE in the joint limit of infinitely many agents and vanishing time step.

Keywords: Lotka–Volterra equations; predator–prey dynamics; Goodwin model; Minsky hypothesis; financial instability; stochastic market models; business cycles; debt–capital dynamics; financial super-predators; Lyapunov stability; transversal stability

1 Introduction

1.1 Background and Motivation

This paper asks one organizing question: how far can the predator–prey formalism be pushed, with full mathematical rigor, as a unifying description of endogenous economic and financial fluctuations? Three new results anchor our answer: a Lyapunov-based stochastic formulation of Minsky's Financial Instability Hypothesis with a closed-form noise-induced energy-drift rate (Theorem 4.4); an instability theorem for a three-species model with financial super-predators, including a closed-form exponent that decides the fate of the debt market (Theorem 4.8); and a mean-field and continuum limit theorem connecting a finite-size stochastic market model to the deterministic Lotka–Volterra dynamics (Theorem 5.1). Sections 4–5 contain these contributions; Sections 2–3 assemble, in self-contained form, the classical apparatus they require.

The mathematical analysis of complex adaptive systems–whether ecological, economic, or financial–reveals a striking family of recurring phenomena: endogenous oscillations, abrupt regime shifts, and multi-scale feedback loops whose qualitative behavior cannot be captured by linear or static equilibrium models. Among the mathematical frameworks developed to describe such behavior, the predator–prey model of Lotka [18] and Volterra [30] occupies a distinguished

position. In its classical formulation, the system comprises two coupled nonlinear ordinary differential equations (ODEs) with four parameters; yet it generates sustained periodic oscillations, continuous dependence on initial conditions with a one-parameter family of periodic orbits, and a characteristic phase-lag between interacting populations that is robustly observed in ecological field data.

The structural analogy between ecological and economic systems is deeper than mere metaphor. In both settings, agents (organisms, firms, financial intermediaries) grow by consuming a shared resource, encounter carrying-capacity constraints, and generate nonlinear feedback operating across multiple timescales. This structural isomorphism provides a rigorous mathematical basis for transferring the predator–prey apparatus to socioeconomic modeling, a research program pursued with increasing analytical sophistication over the past five decades.

1.2 Related Work

The seminal application of predator–prey dynamics to economics is due to Goodwin [10], who embedded the Lotka–Volterra structure within a one-sector macroeconomic model of growth and income distribution. In Goodwin's formulation, the employment rate and the wage share of output evolve as predator–prey variables, generating endogenous business cycles without any exogenous shock mechanism. Empirical tests of this model for ten OECD economies were conducted by Harvie [12], who documented quantitative agreement between the model's predictions and observed counter-cyclical profit-share dynamics. Extensions incorporating nonlinear investment functions were developed by Desai et al. [6], who showed that a convex investment response breaks the conservative center of the classical system and can generate either a globally attracting limit cycle or damped oscillations, depending on the curvature of the investment function. System-dynamics applications of three-trophic-level predator–prey models to industrial supply chains were carried out by Crookes and Blignaut [5], with quantitative calibration to South African steel industry data.

In financial economics, the predator–prey framework has been applied to buyer–seller order-flow dynamics by Montero [22], who demonstrated that stochastic perturbations of the Lotka–Volterra buyer–seller system generate fat-tailed return distributions consistent with empirical equity-market data. The connection between predator–prey dynamics and Minsky's Financial Instability Hypothesis [21] was developed by Keen [15], who calibrated a debt–capital model to US data for 1945–2007 and demonstrated that the ratio of private debt to GDP follows a destabilizing trajectory in the decade preceding the 2008 financial crisis. Closely related, Asada [2] formulates a Lotka–Volterra predator–prey model of Minsky's hypothesis with private debt as predator and income as prey, including stability analysis and policy extensions. On the stochastic side, Shaikhet and Korobeinikov [28] obtain sharp sufficient conditions for stochastic extinction and persistence of a perturbed Lotka–Volterra predator–prey model via the direct Lyapunov method. The role of highly leveraged speculative intermediaries as a destabilizing third trophic level was analyzed by Goldstein [9] (a working paper), who introduced the concept of *financial super-predators* and provided qualitative stability analysis. On the computational side, agent-based models (ABMs) of financial markets developed by Lux and Marchesi [19] and Chiarella et al. [4] demonstrate that heterogeneous trend-following and fundamentalist agents generate volatility clustering, fat-tailed returns, and herd-driven price cycles without requiring exogenous news shocks.

Despite this active literature, several gaps motivate the present work. First, the global (Lyapunov) stability analysis of the debt–capital model, and a careful treatment of the noise-induced energy drift in its stochastic perturbation, have received less attention than local linearization. Second, informal claims that an inequality between the debt-side and capital-side rates (r_D versus r_C) governs Minskyan instability have not been reconciled with the fact that a genuine Lotka–Volterra predator–prey system is a neutral center for *all* positive parameters; we clarify the correct stochastic statement. Third, while the three-population Hopf-to-chaos route is established in the ecological literature [8, 31], its financial interpretation through a super-predator (third trophic) layer has not been developed. Fourth, finite-size stochastic generalizations of the buyer–seller model would benefit from an explicit mean-field convergence result, formulated with the correct density scaling and a careful separation of the large-population and small-time-step limits. Our contribution is therefore primarily one of *unification and financial interpretation* across these settings rather than wholly new dynamical-systems theory. To be fully explicit about the demarcation between new and known material: Propositions 2.1–2.5 and 3.2 are classical results (or minor reorganizations thereof) included for self-containedness, and Table 1 surveys established applications; the new analytical content of this paper is confined to Theorems 4.4, 4.8 and 5.1, the supporting Proposition 4.7, and their corollaries.

The present study systematically addresses all four identified gaps. Our specific contributions can be summarized as follows.

(C1) Rigorous Lyapunov-based formulation of the debt–capital model. Building on the predator–prey treatments of Minsky's hypothesis by Asada [2] and Keen [15], we construct an explicit first integral / Lyapunov function for the two-species debt–capital ODE and establish three results that, to our knowledge, are new in this setting: (i) the deterministic system is a neutrally stable center for *all* positive parameters (Theorem 4.4(i)–(ii)), so that—correcting the informal "$r_D > r_C$" threshold reading—no deterministic stability threshold exists; (ii) under Itô perturbations the expected energy drifts strictly outward at the closed-form rate $\frac{1}{2}(\sigma_C^2 r_D + \sigma_D^2 r_C) > 0$ (Theorem 4.4(iv)), a quantitative measure of noise-induced Minskyan fragility; and (iii) the ratio r_C/r_D governs equilibrium leverage and

the direction of noise-driven excursions rather than deterministic stability. This provides a clean Lyapunov-based statement of Minsky's Financial Instability Hypothesis.

(C2) Three-species super-predator model: equilibrium, instability, and extinction criterion. We establish the existence and uniqueness of a positive interior equilibrium under an explicit parameter condition (Proposition 4.7), prove that this equilibrium is *unstable for all positive parameter values*—so that stable interior coexistence of capital, debt, and super-predators is impossible in this model—and derive a closed-form transversal Floquet exponent λ_D, uniform across all boundary cycles, that decides whether debt is driven to extinction (Theorem 4.8). The financial interpretation of the third trophic layer and the resulting unconditional instability mechanism are the novel contributions.

(C3) Mean-field and continuum limit for the finite-size stochastic market model. We prove a two-step limit theorem (Theorem 5.1) for a finite-size stochastic buyer–seller market model with explicit density-dependent scaling: at fixed time step Δt, the size-N process converges in probability, with an explicit $O(1/N)$ mean-square bound, to the deterministic Euler map; and in the joint limit $N \to \infty$, $\Delta t \to 0$ it converges in probability, uniformly on compact time intervals, to the deterministic Lotka–Volterra ODE. This places the finite-N fluctuations responsible for fat tails and volatility clustering on a firm asymptotic footing while keeping the discrete-time and continuous-time limits carefully separated.

(C4) Unified policy framework. We translate the structural parameters of each model into explicit policy instruments—wage floors, leverage caps, transaction taxes, circuit breakers—and characterize, via the stability criteria established in (C1)–(C2), the direction and magnitude of their effects on the equilibrium stability of each system.

The remainder of the paper is organized as follows. Section 2 presents the Lotka–Volterra framework, establishes positive invariance and the Hamiltonian conservation law, and analyzes the Rosenzweig–MacArthur logistic extension, the two-species competition model, and the reaction–diffusion generalization. Section 3 develops the economic applications: the Goodwin growth-cycle model (with an isomorphism proof), the Desai–Henry–Mosley–Pemberton investment-accelerator extension, and the three-trophic sectoral model. Section 4 presents the financial applications: the buyer–seller asset-price model, the debt–capital model with Lyapunov analysis and the Minsky criterion, and the three-species super-predator system. Section 5 formulates the finite-size stochastic market model, states the mean-field and continuum limit theorem, and collects reproducibility and sensitivity information for the numerical experiments. Section 6 discusses policy implications. Section 7 summarizes the main mathematical findings and outlines directions for future research. All proofs are placed immediately after the corresponding statements.

2 The Lotka–Volterra Framework and Its Principal Extensions

2.1 The Classical Two-Species Model

Let $x(t) > 0$ denote the prey population density and $y(t) > 0$ the predator population density at time $t \geq 0$. The classical Lotka–Volterra predator–prey system is

$$\frac{dx}{dt} = rx - axy, \tag{1a}$$

$$\frac{dy}{dt} = -my + bxy, \tag{1b}$$

where all parameters satisfy r, a, m, $b > 0$. The ecological interpretations are standard:
- r: intrinsic per-capita growth rate of the prey in the absence of predation;
- a: per-capita predation rate (encounter rate multiplied by kill probability);
- m: per-capita mortality rate of the predator in the absence of prey;
- b: biomass conversion efficiency from consumed prey to new predator biomass.

The right-hand side of (1) is of class C^∞ on $\mathbb{R}^2$, and hence locally Lipschitz. By the Picard–Lindelöf theorem, for every initial condition $(x_0, y_0) \in \mathbb{R}^2_{>0}$ there exists a unique maximal solution. The following proposition establishes that this solution is, in fact, global.

Proposition 2.1 (Positive invariance and global existence)**.** *For every initial condition $(x_0, y_0) \in \mathbb{R}^2_{>0}$, the unique solution $(x(t), y(t))$ of (1) remains in $\mathbb{R}^2_{>0}$ for all $t \geq 0$ and exists for all finite time.*

Proof. On the invariant boundary ray $\{x = 0,\, y > 0\}$ one has $\dot{x} = 0$, and on $\{y = 0,\, x > 0\}$ one has $\dot{y} = 0$. Hence the coordinate axes are forward-invariant, which prevents any trajectory starting in $\mathbb{R}^2_{>0}$ from reaching the boundary in finite time. Boundedness of the maximal solution on compact time intervals follows from the first integral established in Proposition 2.2 below, which shows that every orbit lies on a compact level set of a coercive function. Global existence then follows from the standard continuation theorem for ODEs [11, Theorem II.3.1]. □

Equilibria and linearization

Setting $\dot{x} = \dot{y} = 0$ yields exactly two equilibria in $\mathbb{R}^2_{\geq 0}$:
1. *Trivial equilibrium:* $E_0 = (0, 0)$.
2. *Interior (coexistence) equilibrium:* $E^* = \big(m/b,\ r/a\big) \in \mathbb{R}^2_{>0}$.
   The Jacobian of the vector field evaluated at E^* is

$$J(E^*) = \begin{pmatrix} 0 & -am/b \\ br/a & 0 \end{pmatrix}, \tag{2}$$

with characteristic polynomial $\lambda^2 + rm = 0$ and eigenvalues $\lambda_{1,2} = \pm i\sqrt{rm}$. Since $\operatorname{tr} J(E^*) = 0$ and $\det J(E^*) = rm > 0$, the linearization classifies E^* as a *center*, which is consistent with (but does not prove) nonlinear neutral stability. Global center stability is established through the following conserved quantity.

Proposition 2.2 (First integral and global center structure)**.** *The function $H\colon \mathbb{R}^2_{>0} \to \mathbb{R}$ defined by*

$$H(x, y) \ = \ bx - m \ln x + ay - r \ln y \tag{3}$$

is a first integral of (1): $\dot{H}(x(t), y(t)) = 0$ for every solution. Moreover, H is strictly convex on $\mathbb{R}^2_{>0}$ with a unique global minimum at E^*, and H is coercive. Consequently, for every $c > H(E^*)$ the sublevel set $\{H \leq c\}$ is a compact, connected region containing E^*, whose boundary (the level set *$\{H = c\}$) is a simple closed curve in $\mathbb{R}^2_{>0}$ surrounding E^*; all orbits of (1) in $\mathbb{R}^2_{>0}$ are periodic and surround E^*.*

Proof. A direct calculation gives

$$\begin{aligned} \frac{dH}{dt} &= \Big(b - \frac{m}{x}\Big)\dot{x} + \Big(a - \frac{r}{y}\Big)\dot{y} \\ &= \Big(b - \frac{m}{x}\Big)(rx - axy) + \Big(a - \frac{r}{y}\Big)(-my + bxy) \\ &= (bx - m)(r - ay) + (ay - r)(-m + bx) \\ &= (bx - m)(r - ay) - (r - ay)(bx - m) \ = \ 0. \end{aligned}$$

Strict convexity of H on $\mathbb{R}^2_{>0}$ follows from the computation $\nabla^2 H = \operatorname{diag}\big(m/x^2,\ r/y^2\big)$, which is positive definite for all $(x, y) \in \mathbb{R}^2_{>0}$. The unique minimum of H is attained at $\nabla H = 0$, i.e., at $(x, y) = (m/b,\ r/a) = E^*$. Compactness of sublevel sets follows from the coercivity of H (i.e., $H(x, y) \to +\infty$ as $x \to 0^+$, $y \to 0^+$, $x \to +\infty$, or $y \to +\infty$). For $c > H(E^*)$ the sublevel set $\{H \leq c\}$ is thus a compact convex region, and its boundary $\{H = c\}$ is a simple closed curve. Since H is constant on every orbit, each orbit lies in a level set; being confined to a compact simple closed curve free of equilibria, every orbit in $\mathbb{R}^2_{>0} \setminus \{E^*\}$ traverses the full curve and is periodic. □

Corollary 2.3 (Period formula near E^*)**.** *The angular frequency of small-amplitude oscillations near E^* is $\omega_0 = \sqrt{rm}$, so the period satisfies*

$$T(\varepsilon) = \frac{2\pi}{\sqrt{rm}}\big(1 + O(\varepsilon^2)\big),$$

where $\varepsilon > 0$ measures the amplitude of the orbit about E^*.

Proof. The linearization (2) has eigenvalues $\pm i\sqrt{rm}$, giving the leading period $2\pi/\sqrt{rm}$. For the order of the correction, pass to the variables $(p, q) = (\ln x, \ln y)$, in which (1) becomes the canonical analytic Hamiltonian system $\dot{p} = -\partial_q \widetilde{H}$, $\dot{q} = \partial_p \widetilde{H}$ with $\widetilde{H}(p, q) = be^p - mp + ae^q - rq$, possessing a nondegenerate minimum h_0 at $(\ln(m/b), \ln(r/a))$. For a one-degree-of-freedom analytic Hamiltonian near a nondegenerate center, the period of the orbit on the energy level h is an analytic function $T(h)$ of h near h_0 (equivalently, in Birkhoff normal form the period depends only on the value of the energy; see [17, Section 8.2]). Since $\widetilde{H} - h_0$ vanishes quadratically at the minimum, an orbit whose amplitude about E^* is of order ε has $h - h_0 = O(\varepsilon^2)$, and therefore

$$T(\varepsilon) = T(h_0) + O(h - h_0) = \frac{2\pi}{\sqrt{rm}}\big(1 + O(\varepsilon^2)\big).$$

In particular the first amplitude correction to the period is of order ε^2; its explicit coefficient follows from the third-order normal form and is not needed here. □

Remark 2.4 (Saddle structure at E_0)**.** *Complementing the forward-invariance of $\mathbb{R}^2_{>0}$ in Proposition 2.1: at $E_0 = (0, 0)$ the Jacobian is* $\operatorname{diag}(r, -m)$*, with eigenvalues $r > 0$ and $-m < 0$, so E_0 is a hyperbolic saddle whose stable manifold is the*

y-axis. Consequently no trajectory originating in the open quadrant $\mathbb{R}^2_{>0}$ approaches E_0 in forward time.

Figure 1 illustrates the time series and phase portrait for the representative parameter set $(r, a, m, b) = (1.0,\ 0.1,\ 0.5,\ 0.05)$ with initial condition $(x_0, y_0) = (10,\ 5)$, giving $E^* = (10,\ 10)$ and $T = 2\pi/\sqrt{0.5} \approx 8.89$.

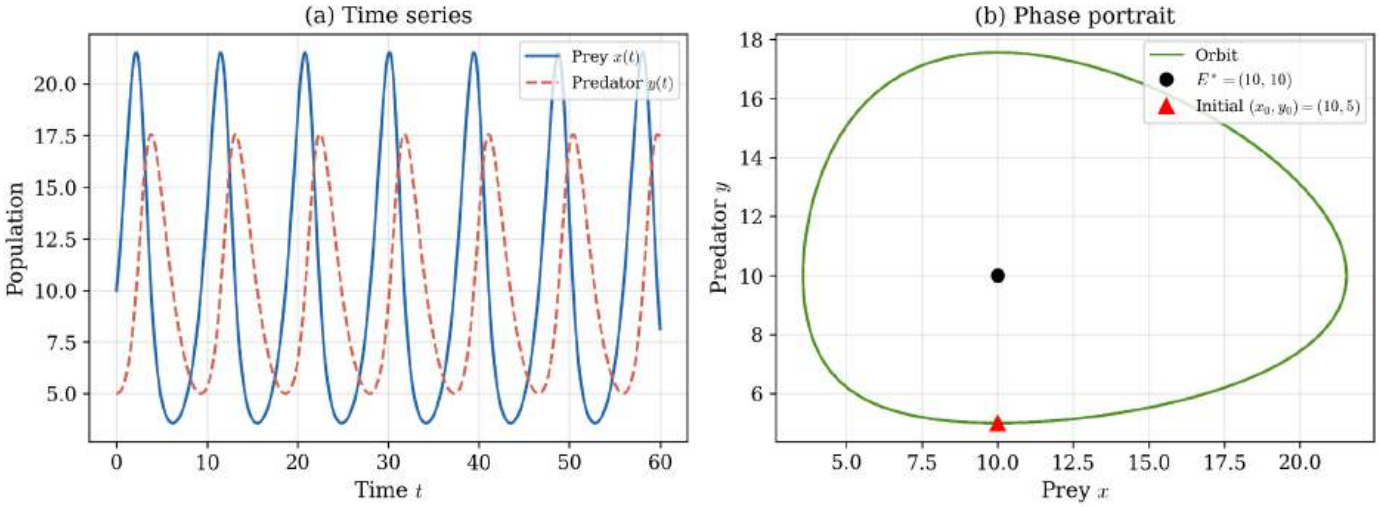


Figure 1. Numerical simulation of the Lotka–Volterra system (1) with $(r, a, m, b) = (1.0, 0.1, 0.5, 0.05)$ and $(x_0, y_0) = (10, 5)$. **(a)** Time series: prey (blue, solid) and predator (red, dashed) exhibit anti-correlated periodic oscillations with period $T = 2\pi/\sqrt{0.5} \approx 8.89$. **(b)** Phase portrait: the closed orbit surrounds the center equilibrium $E^* = (10, 10)$ (filled circle), confirming the conservative structure established in Proposition 2.2.

2.2 Extension I: Logistic Prey Growth (Rosenzweig–MacArthur Model)

The basic model (1) assumes both that the prey population grows without bound in the absence of predation and that predators consume prey at a rate linear in prey density. Both idealizations are ecologically unrealistic. Imposing a prey carrying capacity $K > 0$ *and* a saturating Holling type II functional response $g(x) = ax/(1 + ahx)$ (with handling time $h > 0$) yields the genuine *Rosenzweig–MacArthur* system:

$$\frac{dx}{dt} = rx\Big(1 - \frac{x}{K}\Big) - \frac{axy}{1 + ahx}, \tag{4a}$$

$$\frac{dy}{dt} = -my + \frac{bxy}{1 + ahx}. \tag{4b}$$

A linear functional response ($h = 0$) does not produce sustained oscillations: the interior equilibrium then has trace $-rm/(bK) < 0$ for all K and is globally attracting. The saturation $h > 0$ is precisely what destabilizes the equilibrium and generates the limit cycle below.

Proposition 2.5 (Hopf bifurcation and paradox of enrichment)**.** *Assume $b > mah$, so that the predator nullcline admits the positive root*

$$x^* = \frac{m}{b - mah},$$

and assume $K > x^*$. Then (4) has a unique interior equilibrium $E^* = (x^*, y^*) \in \mathbb{R}^2_{>0}$ with $y^* = \frac{r}{a}\big(1 - \frac{x^*}{K}\big)\big(1 + ahx^*\big)$. Let

$$x_M = \tfrac{1}{2}\big(K - \tfrac{1}{ah}\big)$$

denote the location of the maximum of the prey nullcline, and set $K_c = 2x^* + \frac{1}{ah}$ (equivalently, K_c is the value of K at which $x_M = x^*$). Then:

(i) *If $K < K_c$ (so $x^* > x_M$, the equilibrium lies on the decreasing branch of the prey nullcline), then E^* is locally asymptotically stable.*
(ii) *At $K = K_c$ ($x^* = x_M$) a Hopf bifurcation occurs.*
(iii) *If $K > K_c$ ($x^* < x_M$), then E^* is unstable and is surrounded by a stable limit cycle (the* paradox of enrichment *[27]).*

Proof. The predator nullcline $-m + bx/(1 + ahx) = 0$ gives $x^* = m/(b - mah)$, independent of K; the prey nullcline $r(1 - x/K) = ay/(1 + ahx)$ then gives y^*, positive iff $x^* < K$. Writing $g(x) = ax/(1 + ahx)$ so that $g'(x) = a/(1 + ahx)^2$,

the Jacobian at E^* is

$$J(E^*) = \begin{pmatrix} r\left(1 - \frac{2x^*}{K}\right) - y^* g'(x^*) & -g(x^*) \\ b\, y^*\, g'(x^*)/a & 0 \end{pmatrix},$$

where the $(2,2)$-entry vanishes because $-m + bx^*/(1+ahx^*) = 0$. Hence $\det J(E^*) = g(x^*)\, b\, y^* g'(x^*)/a > 0$, so E^* is nondegenerate, and $\operatorname{tr} J(E^*)$ equals the $(1,1)$-entry. Using $y^* a/(1+ahx^*) = r(1 - x^*/K)$ from the prey nullcline,

$$\operatorname{tr} J(E^*) = r\left(1 - \frac{2x^*}{K}\right) - \frac{r\,(1 - x^*/K)}{1 + ahx^*},$$

which vanishes exactly when $x^* = x_M = \frac{1}{2}(K - 1/(ah))$, i.e. at $K = K_c$; it is negative for $K < K_c$ (so E^* is stable) and positive for $K > K_c$ (so E^* is unstable). At $K = K_c$ the eigenvalues are purely imaginary, and $\partial_K[\operatorname{tr} J]_{K=K_c} \neq 0$ since x_M is strictly increasing in K while x^* is fixed, verifying the transversality condition. The sign of the first Lyapunov coefficient, which determines super- versus subcriticality of the bifurcating cycle, may be computed by the standard formula in [17, Section 8.2] and is generically negative, giving the stable limit cycle of case (iii). □

2.3 Extension II: Two-Species Lotka–Volterra Competition

For two species competing for a common resource, the Lotka–Volterra competition model takes the form

$$\frac{dx_1}{dt} = r_1 x_1 \left(1 - \frac{x_1 + \alpha_{12} x_2}{K_1}\right), \tag{5a}$$

$$\frac{dx_2}{dt} = r_2 x_2 \left(1 - \frac{x_2 + \alpha_{21} x_1}{K_2}\right), \tag{5b}$$

where $\alpha_{12} > 0$ (respectively $\alpha_{21} > 0$) is the per-capita competitive effect of species 2 (respectively species 1). The long-time behavior of (5) is determined entirely by the geometry of the two nullclines: stable coexistence occurs if and only if $\alpha_{12}\alpha_{21} < 1$ together with $K_1/\alpha_{12} > K_2$ and $K_2/\alpha_{21} > K_1$; otherwise one species excludes the other (competitive exclusion principle) [23, Chapter 3].

2.4 Extension III: Reaction – Diffusion Generalization

Incorporating random dispersal over a bounded spatial domain $\Omega \subset \mathbb{R}^n$ (with smooth boundary $\partial\Omega$) yields the reaction–diffusion system

$$\frac{\partial x}{\partial t} = rx\left(1 - \frac{x}{K}\right) - \frac{axy}{1+ahx} + D_x \nabla^2 x, \qquad (z,t) \in \Omega \times (0,\infty), \tag{6a}$$

$$\frac{\partial y}{\partial t} = -my + \frac{bxy}{1+ahx} + D_y \nabla^2 y, \tag{6b}$$

with Neumann boundary conditions $\partial_n x = \partial_n y = 0$ on $\partial\Omega$, where $D_x, D_y > 0$ are diffusion coefficients and ∇^2 denotes the Laplace–Beltrami operator on Ω. The spatially uniform equilibrium corresponding to E^* of Proposition 2.5 can become unstable with respect to spatially heterogeneous perturbations when $D_y \gg D_x$, generating stationary Turing patterns even when E^* is linearly stable in the spatially homogeneous ODE [24, Chapter 2]. In the economic context analyzed in Section 3.3, such diffusion-driven instabilities correspond to the spatial concentration and clustering of industrial productive activity.

3 Predator-Prey Models in Economics

3.1 The Goodwin Growth-Cycle Model

The model of Goodwin [10] embeds the Lotka–Volterra structure within a one-sector macroeconomic growth model under the following structural assumptions.

Assumption 3.1 (Goodwin model hypotheses)**.** (G1) *The capital–output ratio $\nu > 0$ is fixed (Leontief technology).*
(G2) *The savings rate $s \in (0,1)$ applies exclusively to profit income.*
(G3) *Labor productivity grows at the exogenous rate $\alpha > 0$, and the labor force grows at the exogenous rate $\beta > 0$.*
(G4) *The real wage adjusts according to the Phillips curve $\phi(v) = -\gamma + \rho v$ for constants $\gamma, \rho > 0$.*

Under Assumption 3.1, define the *wage share* and *employment rate*:

$$\omega(t) \;\equiv\; \frac{w(t)L(t)}{Y(t)} \in (0,1), \qquad v(t) \;\equiv\; \frac{L(t)}{N(t)} \in (0,1), \tag{7}$$

where w, L, Y, and N denote, respectively, the real wage, employment, aggregate output, and labor force. Standard

manipulations of the national-income accounting identities yield the following system (see [10, 12] for derivation):

$$\frac{d\omega}{dt} = \omega\big[\phi(v) - \alpha\big] = \omega\big[-(\gamma+\alpha) + \rho v\big], \tag{8a}$$

$$\frac{dv}{dt} = v\left[\frac{s(1-\omega)}{\nu} - (\alpha+\beta)\right], \tag{8b}$$

where $\alpha > 0$ is the rate of labor-productivity growth introduced in Assumption 3.1 (G3); we use the single symbol α for this primitive throughout.

Proposition 3.2 (Algebraic isomorphism with Lotka–Volterra)**.** *Under Assumption 3.1 and the hypothesis $s/\nu > \alpha + \beta$ (i.e., the warranted growth rate exceeds the natural growth rate), system (8) is algebraically identical to (1) under the parameter correspondence*

$$x \leftrightarrow v, \quad y \leftrightarrow \omega, \quad r \leftrightarrow \tfrac{s}{\nu} - (\alpha+\beta), \quad a \leftrightarrow \tfrac{s}{\nu}, \quad m \leftrightarrow \gamma + \alpha, \quad b \leftrightarrow \rho. \tag{9}$$

Consequently, the system (8) admits the first integral

$$H_{\mathrm{GW}}(v,\omega) = \tfrac{s}{\nu}\, v - (\gamma+\alpha)\ln v + \tfrac{s}{\nu}\,\omega - \big[\tfrac{s}{\nu} - (\alpha+\beta)\big]\ln\omega, \tag{10}$$

and every orbit in $(v,\omega) \in (0,1)^2$ is a closed curve surrounding the unique interior equilibrium

$$v^* = \frac{\gamma+\alpha}{\rho}, \qquad \omega^* = 1 - \frac{(\alpha+\beta)\nu}{s}. \tag{11}$$

Proof. Direct substitution of the correspondence (9) into (1) recovers (8) exactly. The existence, uniqueness, and positivity of the interior equilibrium (11) follow from the parameter conditions imposed. The first integral (10) is then the Hamiltonian (3) under the same substitution; its strict convexity and the periodicity of all orbits follow from Proposition 2.2. □

Economic interpretation

The Goodwin mechanism operates through the following four-phase closed feedback loop, which requires no exogenous shocks (see [6, 12]):

1. High profit share ⇒ rapid capital accumulation ⇒ rising employment rate v.
2. Rising v ⇒ tighter labor markets ⇒ rising wage share ω.
3. Rising ω ⇒ profit share compressed ⇒ investment falls ⇒ v declines.
4. Falling v ⇒ wage demands moderate ⇒ ω falls ⇒ profit share recovers.

Figure 2 presents a numerical simulation of (8) for the parameter values $\alpha = 0.03$, $\beta = 0.02$, $\rho = 1/15 \approx 0.0667$, $\gamma = 0.03$, $s = 0.8$, $\nu = 3.0$, $(v_0, \omega_0) = (0.90, 0.79)$. With these values, (11) gives the interior equilibrium $E^* = (v^*, \omega^*) = (0.900, 0.8125)$, and the small-amplitude period is $T = 2\pi/\sqrt{rm} \approx 55$ years.

3.2 Extension: Investment Accelerator and Hopf Bifurcation

Desai et al. [6] replace the linear savings function in (8) with a nonlinear investment function $I\colon (0,1) \to \mathbb{R}_{>0}$ that responds to the profit share $\pi = 1 - \omega$:

$$\frac{d\omega}{dt} = \omega\big[\phi(v) - (\alpha + \pi_0)\big], \tag{12a}$$

$$\frac{dv}{dt} = v\left[\frac{I(1-\omega)}{\nu} - (\alpha+\beta)\right]. \tag{12b}$$

A strictly convex function $I(\cdot)$ (i.e., $I'' > 0$) introduces asymmetric nonlinearity that generically destroys the conservative center structure of (8). Depending on the sign of the first Lyapunov coefficient at the Hopf bifurcation point, the system either possesses a globally attracting limit cycle (supercritical case) or exhibits a locally unstable limit cycle surrounding a stable equilibrium (subcritical case). This richer dynamical behavior is more consistent with the empirically observed amplitude variation across business cycles [6].

3.3 Three-Trophic Sectoral Model

Crookes and Blignaut [5] apply a three-trophic-level predator–prey model to the South African industrial supply chain, in which the automotive sector (top predator) depends on steel (mesopredator), which in turn depends on iron ore (primary prey). Denoting iron ore output, steel production, and automotive output by $I(t)$, $S(t)$, and $A(t)$, respectively,

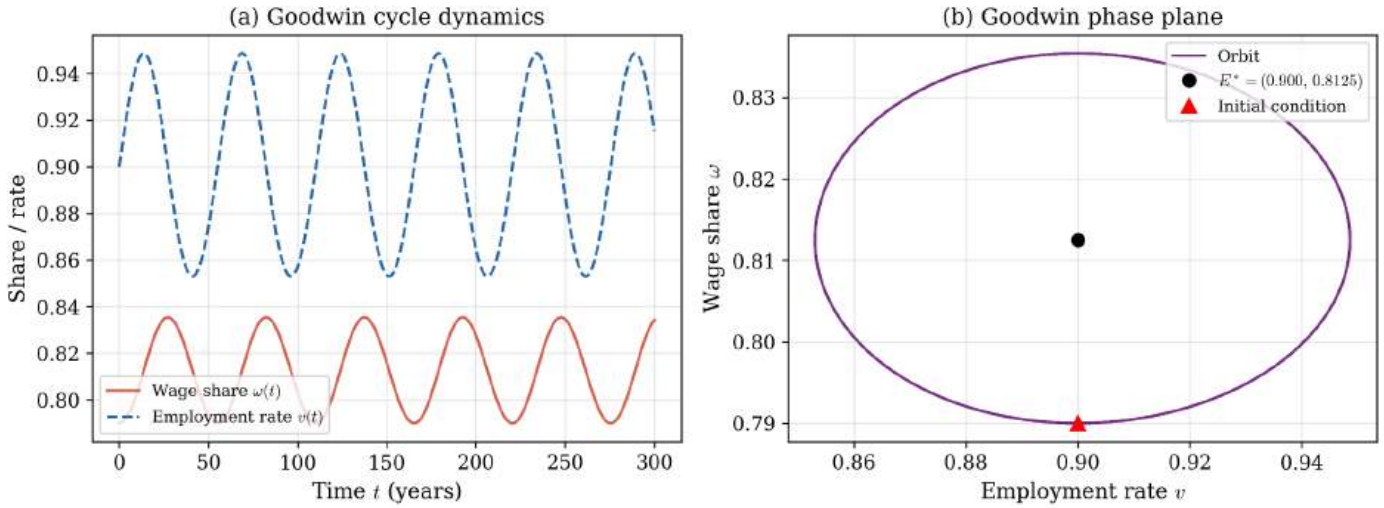


Figure 2. Numerical simulation of the Goodwin model (8) with $\alpha = 0.03$, $\beta = 0.02$, $\rho = 1/15 \approx 0.0667$, $\gamma = 0.03$, $s = 0.8$, $\nu = 3.0$, and $(v_0, \omega_0) = (0.90, 0.79)$. With these parameters, (11) yields $E^* = (v^*, \omega^*) = (0.900,\ 0.8125)$, which is the center about which the orbit closes. **(a)** Time series: the employment rate (blue, dashed) leads the wage share (red, solid) by approximately a quarter-period, reproducing the counter-cyclical profit-share dynamics documented in OECD data by Harvie [12]. **(b)** Phase portrait: the closed orbit in the (v, ω)-plane surrounds the center equilibrium (11) (filled circle), confirming the conservative Lotka–Volterra structure established in Proposition 3.2.

the system is:

$$\frac{dI}{dt} = r_I I - a_{IS} IS, \tag{13a}$$

$$\frac{dS}{dt} = -m_S S + b_{IS} IS - a_{SA} SA, \tag{13b}$$

$$\frac{dA}{dt} = -m_A A + b_{SA} SA, \tag{13c}$$

where all parameters are positive. Calibration of (13) to South African production indices for the period 1970–2010 yielded goodness-of-fit $R^2 > 0.85$ for the cyclical component [5], confirming the quantitative applicability of the trophic-cascade interpretation to industrial supply chains. We include this three-trophic model not as a new contribution but as a building block: it establishes the three-species predator–prey template that the financial super-predator system of Section 4.3 adapts to the debt–capital–intermediary setting.

Table 1. Predator–prey mappings in the economic applications of this paper. All models in rows 1–4 are derived or surveyed in Sections 3 and 4.

Model	Prey	Predator	Key analytical result
Goodwin [10]	Employment rate v	Wage share ω	Conservative center; Prop. 3.2
Desai et al. [6]	Employment v	Wage share ω	Hopf bifurcation; limit cycles
Crookes and Blignaut [5]	Iron ore / Steel	Steel / Automotive	Sectoral margin cycles; $R^2 > 0.85$
Addison et al. [1]	Buying stock B	Selling stock S	Oscillatory asset returns

4 Financial Market Applications

4.1 Buyer–Seller Dynamics and Asset Prices

We recall the buyer–seller model of Montero [22] (a preprint) not as a new result but because it is the deterministic backbone of the finite-size stochastic market model analyzed in Section 5, where our mean-field convergence theorem (Theorem 5.1) is the novel contribution. Montero [22] models a financial market as a two-species Lotka–Volterra system in

which the aggregate population of buyers $B(t) > 0$ and sellers $S(t) > 0$ interact as prey and predator, respectively:

$$\frac{dB}{dt} = r_B B - a_{BS} BS, \tag{14a}$$

$$\frac{dS}{dt} = -m_S S + b_{BS} BS. \tag{14b}$$

By the isomorphism established in Proposition 2.2 (applied with $x \leftrightarrow B$, $y \leftrightarrow S$, $r \leftrightarrow r_B$, $a \leftrightarrow a_{BS}$, $m \leftrightarrow m_S$, $b \leftrightarrow b_{BS}$), all orbits of (14) in $\mathbb{R}^2_{>0}$ are closed, with interior equilibrium

$$B^* = \frac{m_S}{b_{BS}}, \qquad S^* = \frac{r_B}{a_{BS}}.$$

The asset price $P(t)$ is coupled to the order imbalance via the standard price-impact equation:

$$\frac{dP}{dt} = \eta\big[B(t) - S(t)\big], \quad \eta > 0, \tag{15}$$

where η is the price-impact coefficient (denoted by a symbol distinct from the eigenvalue λ used elsewhere). Since $B(t) - S(t)$ oscillates periodically with angular frequency $\omega_0 = \sqrt{r_B m_S}$, the price $P(t)$ oscillates with the same fundamental frequency; the buyer and seller populations are a quarter-cycle out of phase, so the joint trajectory $(B(t), S(t), P(t))$ is a closed, non-planar periodic curve in $\mathbb{R}^3_{>0}$. (We avoid the term "Lissajous", which strictly denotes superposed sinusoids; Lotka–Volterra cycles are periodic but anharmonic.)

Remark 4.1 (Stochastic perturbations and fat-tailed returns)**.** *Multiplicative noise of intensity $\sigma > 0$ applied to (14) destroys the neutrally stable center and produces a diffusing process. Numerical evidence in [22] demonstrates that the resulting price process generates return distributions with excess kurtosis in the range $[3, 7]$, consistent with empirically documented fat tails for daily returns on major equity indices. The rigorous stochastic generalization is developed in Section 5.*

4.2 Debt–Capital Dynamics and the Minsky Hypothesis

Economic background

Minsky's Financial Instability Hypothesis [21] asserts that endogenous financial fragility accumulates during periods of sustained economic expansion: firms migrate from *hedge finance* (cash flows cover all debt obligations), through *speculative finance* (cash flows cover interest but not principal), to *Ponzi finance* (cash flows cover neither), until a *Minsky moment*—a sudden debt-deflation crisis—occurs. This narrative has a natural formalization as a predator–prey ODE, as developed below.

Model derivation from first principles

Let $C(t) > 0$ denote the aggregate stock of productive (non-financial) capital and $D(t) > 0$ the aggregate stock of outstanding debt (bonds, loans, and leveraged positions). We impose the following structural assumptions.

Assumption 4.2 (Debt–capital model)**.** (DC1) *(Autonomous capital growth). In the absence of debt, capital grows at the net rate $r_C > 0$ (gross return less depreciation).*

(DC2) *(Autonomous debt contraction). In the absence of productive capital to finance, the debt stock* contracts *at the net rate $r_D > 0$ (amortization and default dominate when there are no profitable assets to lend against).*

(DC3) *(Predatory interaction on capital). Each unit of debt–capital interaction reduces the net rate of capital accumulation by $a_{DC} > 0$, reflecting debt-service obligations that crowd out investment.*

(DC4) *(Debt feeds on capital). Each unit of debt–capital interaction* increases *the net rate of debt expansion by $b_{DC} > 0$, reflecting the tendency of profitable capital to attract new lending.*

Remark 4.3. *Under Assumption 4.2, the debt–capital interaction reduces $\dot{C}$ (via debt service crowding out investment) while it* increases *$\dot{D}$ (profitable capital attracting new lending). This is the genuine predator–prey sign structure, placing D in the role of predator and C in the role of prey, consistently with [15]. We note in passing that the alternative* competition*-type specification, in which the interaction reduces both $\dot{C}$ and $\dot{D}$, does* not *admit a Lotka–Volterra first integral and is therefore rejected on sign-structure grounds; the predator–prey form below is the appropriate model.*

Under Assumption 4.2, the debt–capital predator–prey system is

$$\dot{C} = r_C\, C - a_{DC}\, CD, \tag{16a}$$

$$\dot{D} = -r_D\, D + b_{DC}\, CD, \tag{16b}$$

with $C(t) > 0$ the stock of productive capital (prey), $D(t) > 0$ the stock of outstanding debt (predator), and parameters $r_C, r_D, a_{DC}, b_{DC} > 0$. Capital grows autonomously at rate r_C and is eroded by debt service through the interaction $a_{DC}CD$; debt *contracts* autonomously at rate r_D (amortization and default dominate in the absence of profitable capital to finance) and *expands* by feeding on capital through $b_{DC}CD$.

Theorem 4.4 (Conservative structure and noise-induced fragility of the debt–capital system)**.** *For system* (16) *with all parameters positive, the following hold.*

(i) ***(Interior equilibrium and center.)*** *The system has a unique interior equilibrium*

$$E^* = (C^*, D^*) = \left(\tfrac{r_D}{b_{DC}}, \tfrac{r_C}{a_{DC}}\right) \in \mathbb{R}^2_{>0},$$

and the Jacobian there is

$$J(E^*) = \begin{pmatrix} 0 & -a_{DC}C^* \\ b_{DC}D^* & 0 \end{pmatrix}, \qquad \operatorname{tr} J(E^*) = 0, \quad \det J(E^*) = r_C r_D > 0,$$

with eigenvalues $\lambda_{1,2} = \pm i\sqrt{r_C r_D}$. Hence E^* is a linear center.

(ii) ***(First integral and global closed-orbit structure.)*** *The function*

$$H(C, D) = b_{DC}\, C - r_D \ln C + a_{DC}\, D - r_C \ln D \tag{17}$$

is a first integral of (16)*: $\dot{H} \equiv 0$ along every solution. Moreover H is strictly convex on $\mathbb{R}^2_{>0}$, with $\nabla^2 H = \operatorname{diag}\big(r_D/C^2,\, r_C/D^2\big) \succ 0$, attains its unique global minimum at E^*, and is coercive. Consequently every orbit of* (16) *in $\mathbb{R}^2_{>0}$ is a closed curve encircling E^*; the equilibrium is Lyapunov stable but not asymptotically stable, and the small-amplitude period is $T = 2\pi/\sqrt{r_C r_D}$.*

(iii) ***(Comparative statics and leverage.)*** *The equilibrium debt level $D^* = r_C/a_{DC}$ is strictly increasing in r_C and strictly decreasing in a_{DC}; the equilibrium capital level $C^* = r_D/b_{DC}$ is strictly increasing in r_D and strictly decreasing in b_{DC}. The equilibrium leverage ratio*

$$\frac{D^*}{C^*} = \frac{b_{DC}\, r_C}{a_{DC}\, r_D}$$

is strictly increasing in r_C and strictly decreasing in r_D.

(iv) ***(Noise-induced fragility: the Minsky mechanism.)*** *Consider the Itô perturbation of* (16)*,*

$$dC = \big(r_C C - a_{DC}CD\big)\, dt + \sigma_C\, C\, dW_t^C, \qquad dD = \big(-r_D D + b_{DC}CD\big)\, dt + \sigma_D\, D\, dW_t^D, \tag{18}$$

where W^C, W^D are independent standard Brownian motions and $\sigma_C, \sigma_D > 0$. Then, for every solution,

$$\frac{d}{dt}\,\mathbb{E}\big[H(C_t, D_t)\big] = \tfrac{1}{2}\big(\sigma_C^2\, r_D + \sigma_D^2\, r_C\big) > 0. \tag{19}$$

The conserved energy of the deterministic center therefore drifts strictly outward under any *noise: the neutral cycles of part* (ii) *are destabilized into ever-larger excursions. Under symmetric noise $\sigma_C = \sigma_D = \sigma$ the drift equals $\frac{1}{2}\sigma^2(r_C + r_D)$, and the excursion is borne disproportionately by the debt coordinate precisely when $r_C > r_D$ (equivalently, when $D^*/C^* > b_{DC}/a_{DC}$), which we identify with the Minskyan high-debt regime.*

Remark 4.5. *Part* (iv) *replaces the informal claim that $r_D > r_C$ is* necessary and sufficient *for instability. A genuine Lotka–Volterra predator–prey system is a neutral center for* all *positive parameters (part* (ii)*), and the stochastic energy drift* (19) *is positive for* all *positive parameters; hence no deterministic r_D-versus-r_C stability threshold exists. The economically meaningful role of r_C relative to r_D is comparative—it governs equilibrium leverage (part* (iii)*) and the direction in which noise-driven excursions predominate (part* (iv)*)—rather than a switch between stable and unstable regimes. We also emphasize the probabilistic scope of part* (iv)*: the drift identity* (19) *concerns the* expectation *of H and does not by itself assert almost-sure outward migration of every sample path; pathwise statements would require a separate analysis of the martingale fluctuations and are not claimed here. The Monte-Carlo experiment of Figure 3(c) corroborates the mean drift.*

Proof. (i) Setting the right-hand sides of (16) to zero gives $C\,(r_C - a_{DC}D) = 0$ and $D\,(-r_D + b_{DC}C) = 0$. In $\mathbb{R}^2_{>0}$ this forces $r_C - a_{DC}D = 0$ and $-r_D + b_{DC}C = 0$, i.e. $D^* = r_C/a_{DC}$ and $C^* = r_D/b_{DC}$, which is unique. Writing

$f_1 = r_C C - a_{DC} CD$ and $f_2 = -r_D D + b_{DC} CD$, the Jacobian is

$$J = \begin{pmatrix} r_C - a_{DC} D & -a_{DC} C \\ b_{DC} D & -r_D + b_{DC} C \end{pmatrix}.$$

At E^* the diagonal entries vanish, leaving the stated antidiagonal form; then $\operatorname{tr} J(E^*) = 0$ and $\det J(E^*) = (a_{DC} C^*)(b_{DC} D^*) = r_D r_C > 0$, so $\lambda^2 + r_C r_D = 0$ and $\lambda_{1,2} = \pm i\sqrt{r_C r_D}$.

(ii) Differentiating (17) along solutions,

$$\dot{H} = \left(b_{DC} - \tfrac{r_D}{C}\right)\dot{C} + \left(a_{DC} - \tfrac{r_C}{D}\right)\dot{D}.$$

Substituting $\dot{C} = C(r_C - a_{DC} D)$ and $\dot{D} = D(b_{DC} C - r_D)$ and absorbing the factors C and D,

$$\dot{H} = (b_{DC} C - r_D)(r_C - a_{DC} D) + (a_{DC} D - r_C)(b_{DC} C - r_D).$$

Since $(a_{DC} D - r_C) = -(r_C - a_{DC} D)$, the two products are negatives of one another, so $\dot{H} \equiv 0$. The Hessian $\nabla^2 H = \operatorname{diag}(r_D/C^2,\, r_C/D^2)$ is positive definite on $\mathbb{R}^2_{>0}$, so H is strictly convex; the first-order condition $\nabla H = 0$ gives $b_{DC} = r_D/C$ and $a_{DC} = r_C/D$, i.e. $(C, D) = E^*$, the unique minimizer. Each coordinate contributes a term of the form $\kappa x - \mu \ln x \to +\infty$ as $x \to 0^+$ or $x \to \infty$, so H is coercive and every sublevel set $\{H \le c\}$ is compact. As H is constant on orbits, each level set $\{H = c\}$, $c > H(E^*)$, is invariant; being the boundary of a compact convex sublevel region of a strictly convex coercive function, it is a simple closed curve around E^*. Hence every orbit in $\mathbb{R}^2_{>0}$ is periodic and encircles E^*; H is a (non-strict) Lyapunov function, giving Lyapunov—but not asymptotic—stability since $\dot{H} = 0$. The small-amplitude period follows from the linear angular frequency $\omega_0 = \sqrt{r_C r_D}$ of part (i), so $T = 2\pi/\sqrt{r_C r_D}$.

(iii) Immediate from $D^* = r_C/a_{DC}$ and $C^* = r_D/b_{DC}$ by partial differentiation, with $D^*/C^* = (r_C/a_{DC})(b_{DC}/r_D) = b_{DC} r_C/(a_{DC} r_D)$.

(iv) Apply Itô's formula to $H(C_t, D_t)$ under (18). Because H has no mixed second derivative and the driving noises are independent,

$$dH = \underbrace{\left(H_C f_1 + H_D f_2\right)}_{=\dot{H}=0} dt + \tfrac{1}{2}\left(H_{CC}\, \sigma_C^2 C^2 + H_{DD}\, \sigma_D^2 D^2\right) dt + H_C\, \sigma_C C\, dW^C + H_D\, \sigma_D D\, dW^D.$$

The deterministic bracket vanishes by part (ii). With $H_{CC} = r_D/C^2$ and $H_{DD} = r_C/D^2$, the Itô correction is state-independent:

$$\tfrac{1}{2}\left(\tfrac{r_D}{C^2}\sigma_C^2 C^2 + \tfrac{r_C}{D^2}\sigma_D^2 D^2\right) dt = \tfrac{1}{2}\left(\sigma_C^2 r_D + \sigma_D^2 r_C\right) dt.$$

The remaining integrals

$$\int_0^t H_C \sigma_C C\, dW^C = \int_0^t (b_{DC} C_s - r_D)\sigma_C\, dW_s^C, \qquad \int_0^t H_D \sigma_D D\, dW^D = \int_0^t (a_{DC} D_s - r_C)\sigma_D\, dW_s^D$$

are martingales: under (18) the processes C_t, D_t admit finite second moments on every compact interval (Lemma 4.6 below), so the integrands lie in $L^2(\Omega \times [0,T])$ and the Itô integrals have zero expectation. Taking expectations therefore yields (19). Since $\sigma_C^2 r_D + \sigma_D^2 r_C > 0$, $\mathbb{E}[H(C_t, D_t)]$ is strictly increasing, i.e. *in expectation* the energy migrates to ever-larger values (equivalently, in mean the process occupies ever-larger sublevel sets of H). Under $\sigma_C = \sigma_D = \sigma$ the rate is $\tfrac{1}{2}\sigma^2(r_C + r_D)$; the local flatness of H in the debt direction near E^* scales as $H_{DD}^{-1/2} = \sqrt{r_C}/a_{DC}$, so the share of the excursion carried by the D-coordinate increases with r_C and dominates the capital excursion when $r_C > r_D$.

□

Lemma 4.6 (Finite second moments)**.** *Let (C_t, D_t) solve (18) from a deterministic initial condition $(C_0, D_0) \in \mathbb{R}^2_{>0}$. Then for every $T > 0$ there is a constant $M_T < \infty$ with $\sup_{0 \le t \le T} \mathbb{E}\left[C_t^2 + D_t^2\right] \le M_T$.*

Proof. For $n \in \mathbb{N}$ let $\tau_n = \inf\{t : C_t + D_t \ge n\}$. On $[0, \tau_n]$, Itô's formula gives $d(C_t^2) = \left(2r_C C_t^2 - 2a_{DC} C_t^2 D_t + \sigma_C^2 C_t^2\right) dt + 2\sigma_C C_t^2\, dW_t^C$, and since $a_{DC} C_t^2 D_t \ge 0$ the capital drift is bounded above by $(2r_C + \sigma_C^2) C_t^2$. The corresponding computation for D_t^2, however, produces the interaction term $+2b_{DC} C_t D_t^2$, whose naive control by Young's inequality introduces a

fourth-order term $C_t^2 D_t^2$ that cannot be dominated by $\mathbb{E}[C_t^2 + D_t^2]$ alone; a pure second-moment Grönwall argument therefore does not close. The estimate is nevertheless valid, and rather than reproving it we import it, with precise scope, from the stochastic Lotka–Volterra literature. The system (18) is exactly of the class treated by Mao et al. [20]: multiplicative (linear) environmental noise on a locally Lipschitz Lotka–Volterra drift. For this class their results establish (a) that solutions started in $\mathbb{R}^2_{>0}$ remain positive and do not explode in finite time almost surely, and (b) that all moments are controlled on compact time intervals, $\sup_{0\le t\le T} \mathbb{E}[C_t^p + D_t^p] < \infty$ for every $p \ge 1$ and $T > 0$; Nguyen and Yin [25] provide sharp refinements of such moment and long-time estimates for stochastic competitive and predator–prey Lotka–Volterra models. We use precisely statement (b) with $p = 2$, which gives the stated bound $M_T < \infty$, while the localisation $\tau_n \to \infty$ a.s. follows from statement (a) together with Fatou's lemma. We emphasize that this lemma is therefore *not* self-contained; its only role is to license the martingale property invoked in the proof of Theorem 4.4(iv). □

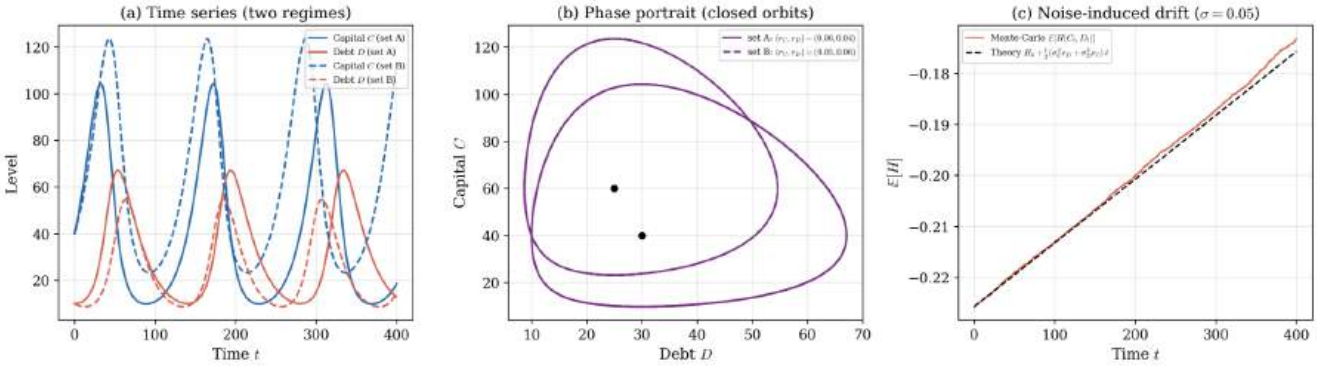


Figure 3. Numerical illustration of the debt–capital predator–prey system (16) and its stochastic perturbation (18), with $(r_C, r_D, a_{DC}, b_{DC}) = (0.06, 0.04, 0.002, 0.001)$ and initial condition $(D_0, C_0) = (10, 40)$. **(a)** Deterministic time series of debt $D(t)$ and capital $C(t)$ for two parameter regimes, illustrating the closed (neutrally stable) cycles guaranteed by Theorem 4.4(ii). **(b)** Phase portrait: every deterministic orbit is a closed curve encircling the interior equilibrium $E^* = (r_D/b_{DC},\, r_C/a_{DC})$ (Theorem 4.4(i)–(ii)). **(c)** Under Itô noise ($\sigma = 0.05$), the expected energy $\mathbb{E}[H(C_t, D_t)]$ drifts strictly outward; the Monte-Carlo estimate (solid) matches the theoretical rate $\frac{1}{2}(\sigma_C^2 r_D + \sigma_D^2 r_C)$ of Theorem 4.4(iv) (dashed), confirming the noise-induced fragility mechanism.

4.3 Three-Species Model: Financial Super-Predators

Motivation

The two-species model (16) captures debt–capital dynamics but abstracts away the role of highly leveraged speculative intermediaries—hedge funds, prime brokers, shadow-banking conduits—which simultaneously extract returns from both productive capital (via collateralized lending and securities financing) and outstanding corporate debt (via securitization and credit-default instruments). These agents constitute a *third trophic level* in the financial ecosystem, which we term *financial super-predators*.

Model formulation

Let $\mathcal{S}(t) > 0$ denote the aggregate activity level of financial super-predators (e.g., total assets under leveraged management, or outstanding repo-market positions). Introducing this third trophic level reorganizes the ecological roles of the first two variables. Whereas in the two-species model (16) debt D is the *predator* feeding on capital, once a super-predator is present both capital C and debt D act as *resources* from which $\mathcal{S}$ extracts returns, while C and D interact competitively. Accordingly C and D each carry autonomous growth and are consumed by $\mathcal{S}$, with $\mathcal{S}$ playing the role of apex predator. We emphasize that the three-species system below is therefore a *distinct* model rather than a direct reduction of (16): setting $\mathcal{S} \equiv 0$ does not recover (16), since the sign of the debt dynamics differs between the two formulations. The three-species system is:

$$\frac{dC}{dt} = r_C C - a_{DC}\, DC - e_{CS}\, C\mathcal{S}, \tag{20a}$$

$$\frac{dD}{dt} = r_D D - b_{DC}\, DC - c_{DS}\, D\mathcal{S}, \tag{20b}$$

$$\frac{d\mathcal{S}}{dt} = -r_{\mathcal{S}}\mathcal{S} + f_{DC}\, DC + g_{CS}\, C\mathcal{S}, \tag{20c}$$

where all parameters $r_C, r_D, r_{\mathcal{S}}, a_{DC}, b_{DC}, e_{CS}, c_{DS}, f_{DC}, g_{CS} > 0$. The term $e_{CS}C\mathcal{S}$ in (20a) represents the rate at which super-predators extract returns from capital (reducing net capital accumulation); $c_{DS}D\mathcal{S}$ in (20b) represents the rate at which super-predators extract returns from debt (reducing net debt expansion); $f_{DC}DC$ and $g_{CS}C\mathcal{S}$ in (20c) represent super-predator growth fueled by debt–capital interactions and direct capital exploitation, respectively. Table 2 collects the notation of this section and of Section 4.2.

Table 2. Notation for the financial models of Section 4. A dash indicates that the symbol does not appear in that model.

Symbol	**Two-species model** (16)	**Three-species model** (20)
r_C	autonomous net growth rate of capital	same
r_D	autonomous contraction rate of debt	autonomous expansion rate of debt
a_{DC}	debt-service drag of the D–C interaction on C	same
b_{DC}	new-lending accrual to D	repayment/deleveraging pressure on D
σ_C, σ_D	noise intensities in (18)	—
$r_{\mathcal{S}}$	—	autonomous decay rate of $\mathcal{S}$
e_{CS}	—	extraction from capital by $\mathcal{S}$
c_{DS}	—	extraction from debt by $\mathcal{S}$
f_{DC}	—	origination margin on D–C interactions accruing to $\mathcal{S}$
g_{CS}	—	direct exploitation of capital by $\mathcal{S}$

Economic microfoundation of the interaction signs

Each bilinear term in (20) embodies a mass-action hypothesis: encounters between two aggregates occur at a rate proportional to the product of their sizes—the same well-mixing idealization used throughout Section 2—and the coefficient measures the value transferred per unit of joint exposure. The economic content of each sign is then as follows. (i) $-a_{DC}DC$ in (20a): exactly as in the two-species model, debt-service obligations crowd out investment in proportion to the joint exposure of debt to capital. (ii) $-b_{DC}DC$ in (20b): in the two-species economy the same interaction *feeds* debt ($+b_{DC}CD$ in (16b)), because banks convert profitable capital into new loans that remain on the measured debt stock. With leveraged intermediaries present, that origination margin is rerouted: securitization and securities financing move newly originated claims off the debt stock D and onto intermediary balance sheets $\mathcal{S}$—captured by the term $+f_{DC}DC$ in (20c)—while amortization and deleveraging pressure on D remain. The net effect of the D–C interaction on D is therefore negative, and the sign reversal relative to (16) is not an ad hoc choice but the accounting counterpart of intermediation: the flow that previously accrued to D now accrues to $\mathcal{S}$. (iii) $-e_{CS}C\mathcal{S}$ and $-c_{DS}D\mathcal{S}$: the super-predator extracts returns from capital (collateralized-lending spreads, securities-financing fees and haircuts) and from debt (securitization spreads, credit-default premia), at rates proportional to its encounters with each resource. (iv) $+f_{DC}DC + g_{CS}C\mathcal{S}$ in (20c): super-predator growth aggregates the intermediation margin on debt–capital origination and the direct exploitation of capital; because part of the extracted value leaks to other sectors (fees, wages, taxes), the growth coefficients need not equal the extraction coefficients. We emphasize that this is a stylized, reduced-form representation: the mapping from $(C, D, \mathcal{S})$ to institutional balance sheets is conceptual, and the purpose of the model is to expose the qualitative consequences of a third trophic layer rather than to provide a calibrated institutional model.

Equilibrium analysis

Setting the right-hand sides of (20) to zero and dividing (20a) and (20b) by $C > 0$ and $D > 0$ respectively, an interior equilibrium $E^{**} = (C^{**}, D^{**}, \mathcal{S}^{**}) \in \mathbb{R}^3_{>0}$ must satisfy

$$r_C = a_{DC}D^{**} + e_{CS}\mathcal{S}^{**}, \qquad r_D = b_{DC}C^{**} + c_{DS}\mathcal{S}^{**}, \qquad r_{\mathcal{S}}\mathcal{S}^{**} = C^{**}\big(f_{DC}D^{**} + g_{CS}\mathcal{S}^{**}\big). \tag{21}$$

The first two conditions express D^{**} and C^{**} as decreasing affine functions of $\mathcal{S}^{**}$,

$$D(\mathcal{S}) = \frac{r_C - e_{CS}\mathcal{S}}{a_{DC}}, \qquad C(\mathcal{S}) = \frac{r_D - c_{DS}\mathcal{S}}{b_{DC}}, \tag{22}$$

positive precisely for $\mathcal{S} < r_C/e_{CS}$ and $\mathcal{S} < r_D/c_{DS}$, respectively. Substituting (22) into the third condition, interior equilibria correspond to roots $\mathcal{S}^{**} \in (0, \bar{\mathcal{S}})$, $\bar{\mathcal{S}} := \min\{r_C/e_{CS}, r_D/c_{DS}\}$, of the quadratic

$$\varphi(\mathcal{S}) := \big(r_D - c_{DS}\mathcal{S}\big)\big[f_{DC}r_C + (a_{DC}g_{CS} - e_{CS}f_{DC})\mathcal{S}\big] - a_{DC}b_{DC}r_{\mathcal{S}}\mathcal{S}. \tag{23}$$

Proposition 4.7 (Existence and uniqueness of the interior equilibrium)**.** *Assume $c_{DS}r_C > e_{CS}r_D$. Then system (20) has exactly one interior equilibrium $E^{**} \in \mathbb{R}^3_{>0}$: $\mathcal{S}^{**}$ is the unique root of φ in $(0, r_D/c_{DS})$, and C^{**}, D^{**} are given by (22).*

Proof. First, $\varphi(0) = r_D f_{DC} r_C > 0$. The assumption $c_{DS} r_C > e_{CS} r_D$ is equivalent to $r_D/c_{DS} < r_C/e_{CS}$, so $\bar{\mathcal{S}} = r_D/c_{DS}$ and $\varphi(\bar{\mathcal{S}}) = -a_{DC} b_{DC} r_{\mathcal{S}} \bar{\mathcal{S}} < 0$. Since φ is a polynomial of degree at most two that is positive at 0 and negative at $\bar{\mathcal{S}}$, it has an odd number of roots, counted with multiplicity, in $(0, \bar{\mathcal{S}})$—hence exactly one. Positivity of C^{**} and D^{**} follows from $\mathcal{S}^{**} < \bar{\mathcal{S}} \le r_C/e_{CS}$ and (22). □

If $c_{DS} r_C \le e_{CS} r_D$ an interior equilibrium may fail to exist; we do not pursue that case. For the parameter set of Figure 4, φ has the unique admissible root $\mathcal{S}^{**} \approx 7.532$, giving $E^{**} \approx (17.404, 22.468, 7.532)$.

Linearization and instability

Writing (20a)–(20b) in Kolmogorov form, $\dot{C} = C(r_C - a_{DC} D - e_{CS} \mathcal{S})$ and $\dot{D} = D(r_D - b_{DC} C - c_{DS} \mathcal{S})$, the per-capita growth rates of C and D vanish at E^{**} by (21); consequently the corresponding diagonal entries of the Jacobian vanish there. Together with $\partial_{\mathcal{S}} \dot{\mathcal{S}}\big|_{E^{**}} = -r_{\mathcal{S}} + g_{CS} C^{**} = -f_{DC} C^{**} D^{**}/\mathcal{S}^{**}$ (again by (21)), the Jacobian of (20) at E^{**} is

$$J(E^{**}) = \begin{pmatrix} 0 & -a_{DC} C^{**} & -e_{CS} C^{**} \\ -b_{DC} D^{**} & 0 & -c_{DS} D^{**} \\ f_{DC} D^{**} + g_{CS} \mathcal{S}^{**} & f_{DC} C^{**} & -\dfrac{f_{DC} C^{**} D^{**}}{\mathcal{S}^{**}} \end{pmatrix}. \tag{24}$$

Its characteristic polynomial is $p(\lambda) = \lambda^3 + p_2 \lambda^2 + p_1 \lambda + p_0$ with $p_2 = -\operatorname{tr} J(E^{**}) = f_{DC} C^{**} D^{**}/\mathcal{S}^{**} > 0$ and $p_0 = -\det J(E^{**})$.

Theorem 4.8 (Instability of interior coexistence and the debt-extinction exponent)**.** *Let all parameters of (20) be positive and assume $c_{DS} r_C > e_{CS} r_D$, so that the interior equilibrium E^{**} of Proposition 4.7 exists and is unique. Then:*

(i) *(No stable interior coexistence.)*

$$\det J(E^{**}) = \frac{C^{**} D^{**}}{\mathcal{S}^{**}} \Big(a_{DC} b_{DC} f_{DC} C^{**} D^{**} + b_{DC} e_{CS} f_{DC} C^{**} \mathcal{S}^{**} + a_{DC} c_{DS} f_{DC} D^{**} \mathcal{S}^{**} + a_{DC} c_{DS} g_{CS} (\mathcal{S}^{**})^2 \Big) > 0, \tag{25}$$

so $p_0 = -\det J(E^{**}) < 0$ and $p(\lambda)$ has a real positive root. Hence E^{**} is unstable for every *choice of positive parameters: no parameter regime renders E^{**} locally asymptotically stable, and no Hopf bifurcation of E^{**} occurs.*

(ii) *(Boundary dynamics.) The face $\{D = 0\}$ is invariant, and on it (20) reduces to the classical Lotka–Volterra pair $\dot{C} = C(r_C - e_{CS} \mathcal{S})$, $\dot{\mathcal{S}} = \mathcal{S}(-r_{\mathcal{S}} + g_{CS} C)$, all of whose orbits in the open face are closed curves around $(\bar{C}, \bar{\mathcal{S}}) = (r_{\mathcal{S}}/g_{CS}, r_C/e_{CS})$ (Proposition 2.2). Along every such closed orbit γ of period T_γ,*

$$\frac{1}{T_\gamma} \oint_\gamma C \, dt = \frac{r_{\mathcal{S}}}{g_{CS}}, \qquad \frac{1}{T_\gamma} \oint_\gamma \mathcal{S} \, dt = \frac{r_C}{e_{CS}}.$$

(iii) *(Uniform transversal exponent.) The transversal Floquet exponent of every boundary orbit γ in the D-direction equals*

$$\lambda_D = r_D - b_{DC} \frac{r_{\mathcal{S}}}{g_{CS}} - c_{DS} \frac{r_C}{e_{CS}}, \tag{26}$$

independently of γ. If $\lambda_D < 0$, every boundary cycle is transversally linearly stable and debt decays exponentially at rate $|\lambda_D|$ near the face; if $\lambda_D > 0$, every boundary cycle is transversally unstable and debt re-invades.

Proof. Part (i). Expanding $\det J(E^{**})$ from (24) along the first row gives (25), a sum of manifestly positive terms (the identity is also readily verified by direct computation). Thus $p(0) = p_0 = -\det J(E^{**}) < 0$ while $p(\lambda) \to +\infty$ as $\lambda \to +\infty$, so p has a real root $\lambda_+ > 0$ and E^{**} has a nontrivial unstable manifold. Equivalently: local asymptotic stability would require all eigenvalues to have negative real parts, which forces $\det J = \lambda_1 \lambda_2 \lambda_3 < 0$ (either three negative real eigenvalues, or one negative real eigenvalue λ_1 and a complex pair $\alpha \pm i\beta$ with $\alpha < 0$, giving $\det J = \lambda_1(\alpha^2 + \beta^2) < 0$); this contradicts (25). Since (25) holds for all positive parameters, no stability boundary—and in particular no Hopf bifurcation of E^{**}—exists.

Part (ii). On $\{D = 0\}$ we have $\dot{D} = 0$, so the face is invariant, and the restricted system is the stated Lotka–Volterra pair, to which Proposition 2.2 applies under the correspondence $(x, y, r, a, m, b) \mapsto (C, \mathcal{S}, r_C, e_{CS}, r_{\mathcal{S}}, g_{CS})$. For the averages, integrate $\frac{d}{dt} \ln \mathcal{S} = -r_{\mathcal{S}} + g_{CS} C$ over one period of γ: periodicity gives $0 = -r_{\mathcal{S}} T_\gamma + g_{CS} \oint_\gamma C \, dt$, i.e. the first identity; the second follows in the same way from $\frac{d}{dt} \ln C = r_C - e_{CS} \mathcal{S}$.

Part (iii). Linearizing the D-equation of (20) about a boundary solution $(C(t), 0, \mathcal{S}(t))$ on γ gives the scalar variational equation $\dot{D} = D\,[\, r_D - b_{DC} C(t) - c_{DS} \mathcal{S}(t) \,]$, so the transversal Floquet multiplier over one period is $\exp\big(\int_0^{T_\gamma} (r_D -$

$b_{DC}C - c_{DS}\mathcal{S})\,dt\big) = \exp(T_\gamma \lambda_D)$ by the averages of part (ii). The value (26) is independent of γ because the averages are. Transversal linear stability (resp. instability) of γ is equivalent to this multiplier being smaller (resp. larger) than one, i.e. to $\lambda_D < 0$ (resp. $\lambda_D > 0$). □

Remark 4.9 (Numerical verification)**.** *For the parameter set of Figure 4, $E^{**} \approx (17.404, 22.468, 7.532)$ and the eigenvalues of (24) are $\{+0.0324,\ -0.0175 \pm 0.0201\,i\}$: a saddle-focus, as guaranteed by part (i). The extinction exponent is $\lambda_D = 0.04 - 0.001 \cdot 20 - 0.003 \cdot 30 = -0.070 < 0$, predicting exponential extinction of debt near the boundary cycles; the empirical decay rate of $\ln D(t)$ in the simulation of Figure 4 over $t \in [200, 550]$ is ≈ -0.075, in agreement with (26).*

Remark 4.10 (Outlook: cyclical and complex dynamics in damped variants)**.** *Theorem 4.8(i) rules out Hopf bifurcations of the interior equilibrium for (20) itself. Damped variants—for instance, logistic self-limitation of capital, which reintroduces a negative diagonal entry in the Jacobian—can in principle support stable coexistence, Hopf bifurcations, and the period-doubling routes to complex dynamics documented for three-species Lotka–Volterra systems by Gardini et al. [8] and classified by Zeeman [31]. Whether a financial super-predator variant of this type exhibits such a route is an open question that we leave for future work; we emphasize that the present model and Figure 4 exhibit no such route (there $\lambda_D < 0$ and the long-run behaviour is a boundary cycle), and we accordingly make no chaos claim for (20).*

Economic implications of Theorem 4.8

1. *No stable coexistence.* The presence of a financial super-predator makes balanced interior coexistence of productive capital, debt, and intermediation structurally impossible: instability of E^{**} holds for *all* positive parameters, in sharp contrast to the two-species model, whose interior equilibrium is a neutral center for all positive parameters (Theorem 4.4). Fragility here is intrinsic to the trophic structure, not a matter of parameter values.
2. *A sharp debt-extinction criterion.* The closed-form exponent (26) decides the fate of the debt market near the boundary regime: ordinary credit survives only if its autonomous expansion rate r_D exceeds $b_{DC}r_{\mathcal{S}}/g_{CS} + c_{DS}r_C/e_{CS}$, the drag exerted through the boundary-cycle averages of capital and super-predator activity.
3. *Wealth concentration.* Equation (20c) shows that $\mathcal{S}$ grows at the expense of both C and D, concentrating financial returns in the shadow-banking sector [9]; in the regime $\lambda_D < 0$ of Figure 4 this culminates in the crowding-out of ordinary credit altogether.

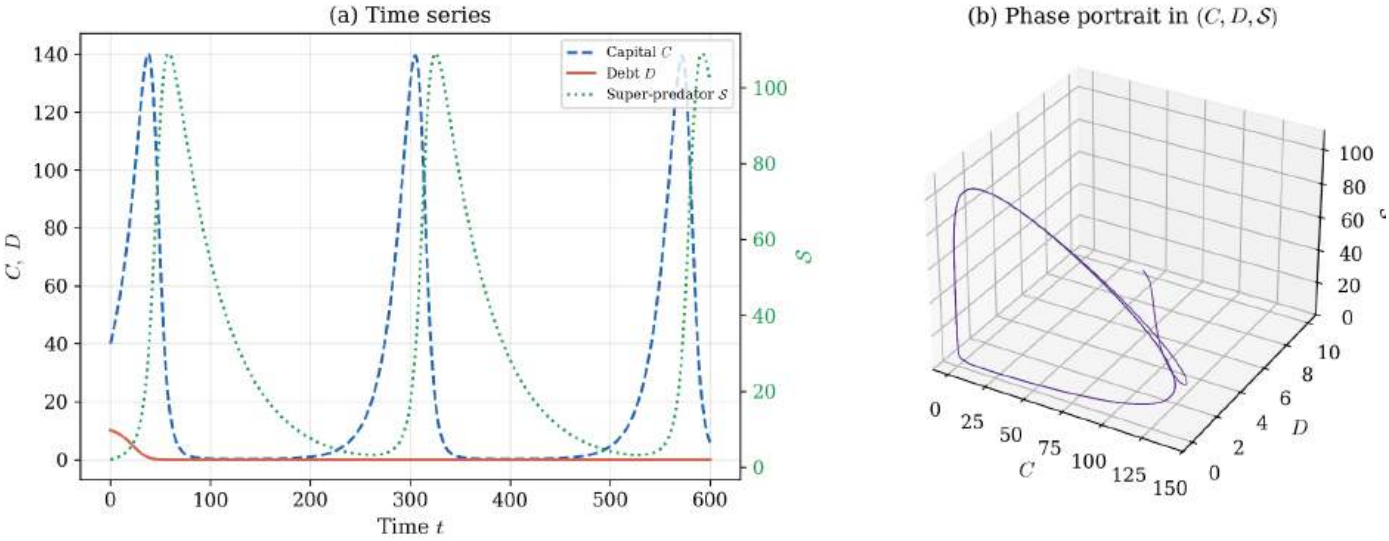


Figure 4. Numerical simulation of the three-species super-predator model (20) with $(r_C, r_D, r_{\mathcal{S}}, a_{DC}, b_{DC}, c_{DS}, e_{CS}, f_{DC}, g_{CS}) = (0.06, 0.04, 0.02, 0.002, 0.001, 0.003, 0.002, 5\times10^{-5}, 0.001)$ and $(C_0, D_0, \mathcal{S}_0) = (40, 10, 2)$, illustrating Theorem 4.8. **(a)** Time series: the interior equilibrium $E^{**} \approx (17.40, 22.47, 7.53)$ is a saddle-focus (Theorem 4.8(i); Remark 4.9), and since $\lambda_D = -0.070 < 0$ (Theorem 4.8(iii)) the debt coordinate D (red, solid, left axis) is driven to extinction at the predicted exponential rate, while capital C (blue, dashed, left axis) and the super-predator $\mathcal{S}$ (green, dotted, right axis) settle onto a neutral Lotka–Volterra cycle of the boundary system on the $D = 0$ face (Theorem 4.8(ii)). The figure should accordingly *not* be read as bounded three-trophic coexistence. **(b)** Corresponding non-planar trajectory in $(C, D, \mathcal{S})$-space, approaching the boundary cycle.

5 Numerical Experiments and Empirical Context

5.1 From Differential Equations to Finite-Size Stochastic Models

Continuous ODE models rest on two key idealizations: (i) perfectly mixing, homogeneous populations (mass-action kinetics) and (ii) a deterministic aggregation that suppresses finite-size fluctuations. Agent-based models (ABMs) relax these idealizations by simulating the discrete decisions of heterogeneous, boundedly rational individuals [3, 7]. The model studied in this section takes a step in that direction at the population level, and we deliberately do *not* call it an agent-based model: it does not track individual agents' states or heterogeneous decision rules. Rather, it is a finite-size *stochastic market model*, the diffusion-scale description of an underlying market of N traders switching between buying and selling at density-dependent rates: aggregate stocks of order N evolve under density-dependent drift, and the $O(1/\sqrt{N})$ noise is the central-limit fluctuation of such a system. The two levels of description are mathematically complementary: the ODE provides closed-form equilibria and Lyapunov results, while the finite-size model quantifies how far a large but finite market deviates from them; Theorem 5.1 makes the connection precise, with the deterministic ODE emerging in the joint limit of infinitely many agents and vanishing time step.

5.2 A Finite-Size Stochastic Market Model with Herding

We formulate a discrete-time stochastic generalization of the buyer–seller model (14) for a market of size N. Let $\Delta t > 0$ be the time step, and let B_t and S_t denote aggregate buying and selling stocks, both of order N. Two explicit scaling assumptions tie the model to the market size. First, mass-action interactions are *density dependent*,

$$a_{BS} = \frac{\alpha_{BS}}{N}, \qquad b_{BS} = \frac{\beta_{BS}}{N}, \tag{27}$$

with $\alpha_{BS}, \beta_{BS} > 0$ fixed as N varies: each unit of buying stock interacts with the *fraction*, not the number, of selling counterparties. Second, aggregate noise has central-limit scale, $\sigma = \sigma_0/\sqrt{N}$ and $\sigma_P = \sigma_P^0/\sqrt{N}$. The model reads

$$B_{t+\Delta t} = B_t + \Delta t\big(r_B(t)B_t - a_{BS}B_tS_t\big) + \sigma B_t\sqrt{\Delta t}\,\varepsilon_t^B, \tag{28a}$$

$$S_{t+\Delta t} = S_t + \Delta t\big(-m_S S_t + b_{BS}B_tS_t\big) + \sigma S_t\sqrt{\Delta t}\,\varepsilon_t^S, \tag{28b}$$

$$P_{t+\Delta t} = P_t\left[1 + \eta\,\Delta t\,\frac{B_t - S_t}{N} + \sigma_P\sqrt{\Delta t}\,\varepsilon_t^P\right], \tag{28c}$$

where $\varepsilon_t^B, \varepsilon_t^S, \varepsilon_t^P \overset{\text{i.i.d.}}{\sim} \mathcal{N}(0,1)$ are independent standard normal shocks and $\eta > 0$ governs price sensitivity to the normalized order imbalance. (With the step $\Delta t = 1$ used in the simulation of Figure 5, the factor Δt in (28c) is immaterial; it matters only for the continuum limit below.) Herding behavior is incorporated by making the buyer growth rate depend on lagged price momentum:

$$r_B(t) = r_B^0 + \kappa\,\frac{P_t - P_{t-1}}{P_{t-1}}, \qquad \kappa \geq 0, \tag{29}$$

where $r_B^0 > 0$ is the baseline growth rate and κ is the trend-following (chartist) coefficient, consistent with empirically documented herding in financial markets [19].

In terms of the *densities* $x_t^{(N)} = B_t/N$ and $y_t^{(N)} = S_t/N$, the scalings (27) turn (28) into

$$x_{t+\Delta t}^{(N)} = x_t^{(N)} + \Delta t\big(r_B(t)x_t^{(N)} - \alpha_{BS}x_t^{(N)}y_t^{(N)}\big) + \frac{\sigma_0}{\sqrt{N}}\,x_t^{(N)}\sqrt{\Delta t}\,\varepsilon_t^B, \tag{30a}$$

$$y_{t+\Delta t}^{(N)} = y_t^{(N)} + \Delta t\big(-m_S y_t^{(N)} + \beta_{BS}x_t^{(N)}y_t^{(N)}\big) + \frac{\sigma_0}{\sqrt{N}}\,y_t^{(N)}\sqrt{\Delta t}\,\varepsilon_t^S, \tag{30b}$$

$$P_{t+\Delta t}^{(N)} = P_t^{(N)}\left[1 + \eta\,\Delta t\,\big(x_t^{(N)} - y_t^{(N)}\big) + \frac{\sigma_P^0}{\sqrt{N}}\sqrt{\Delta t}\,\varepsilon_t^P\right], \tag{30c}$$

whose drift part is precisely the explicit Euler discretization, with step Δt, of the ODE system

$$\dot{x} = r_B^0 x - \alpha_{BS}xy, \qquad \dot{y} = -m_S y + \beta_{BS}xy, \qquad \dot{P} = \eta P\,(x - y). \tag{31}$$

The (x, y) subsystem is the buyer–seller Lotka–Volterra system (14) in density variables; the multiplicative price equation is the density-scaled counterpart of the price-impact rule (15), formulated in relative changes so that P remains positive.

Two distinct limits are therefore in play, and we keep them separate. As $N \to \infty$ at *fixed* Δt, the noise vanishes and the natural deterministic limit is the Euler map, *not* the continuous-time ODE; the ODE (31) is recovered only in the additional limit $\Delta t \to 0$. The following theorem, the third novel analytical contribution of this paper, makes both steps precise.

Theorem 5.1 (Mean-field and continuum limit of the stochastic market model)**.** *Assume $\kappa = 0$ (no herding), the density scaling (27), and the noise scaling $\sigma = \sigma_0/\sqrt{N}$, $\sigma_P = \sigma_P^0/\sqrt{N}$. Fix $T > 0$ and an initial condition $(x_0, y_0, P_0) \in \mathbb{R}^3_{>0}$ independent of N. Let $z_k^{(N)} = (x_{k\Delta t}^{(N)}, y_{k\Delta t}^{(N)}, P_{k\Delta t}^{(N)})$ denote the stochastic process (30), let $\bar z_k = (\bar x_k, \bar y_k, \bar P_k)$ denote the deterministic Euler iterates of (31) with step Δt from the same initial condition, and let $z(t) = (x(t), y(t), P(t))$ denote the solution of (31). Then there exist $\Delta t_0 > 0$ and constants $C_1(T), C_2(T) < \infty$ such that for all $\Delta t \in (0, \Delta t_0]$:*

(i) *(Law of large numbers at fixed Δt.)* $\max\limits_{0\le k\le \lfloor T/\Delta t\rfloor} \mathbb{E}\big[\,\big\|z_k^{(N)} - \bar z_k\big\|^2\,\big] \le \dfrac{C_1(T)}{N}$, *and consequently, for fixed Δt,* $\max_{k\le\lfloor T/\Delta t\rfloor}\big\|z_k^{(N)} - \bar z_k\big\| \to 0$ *in probability as $N \to \infty$.*

(ii) *(Continuum limit of the Euler map.)* $\max\limits_{0\le k\le \lfloor T/\Delta t\rfloor} \|\bar z_k - z(k\Delta t)\| \le C_2(T)\,\Delta t$.

(iii) *(Joint limit.) For every sequence $\Delta t_N \to 0$ with $N\Delta t_N \to \infty$,*

$$\max_{0\le k\le \lfloor T/\Delta t_N\rfloor} \big\|z_k^{(N)} - z(k\Delta t_N)\big\| \longrightarrow 0 \quad \text{in probability as } N \to \infty.$$

In this precise sense the deterministic Lotka–Volterra dynamics (31) are the joint large-N, small-Δt limit of the stochastic market model, while at fixed Δt the limit is the deterministic Euler map.

Proof. Throughout, $(x(t), y(t))$ lies on a closed Lotka–Volterra orbit (Proposition 2.2 applied to (31)) and $P(t) = P_0 \exp\big(\eta \int_0^t (x - y)\,ds\big)$ is bounded and bounded away from zero on $[0, T]$; fix a compact set $K \subset \mathbb{R}^3_{>0}$ containing a ρ-neighbourhood, $\rho > 0$, of $\{z(t) : t \in [0, T]\}$, and let L be a Lipschitz constant on K for the drift map $F(x, y, P) = (r_B^0 x - \alpha_{BS} xy,\ -m_S y + \beta_{BS} xy,\ \eta P(x - y))$.

Part (ii). This is the classical convergence estimate for the explicit Euler method applied to the locally Lipschitz, C^1 vector field F: while the exact solution remains in K, the local truncation error per step is $O(\Delta t^2)$, and the discrete Grönwall inequality propagates it to a global error $C_2(T)\Delta t$ over $\lfloor T/\Delta t\rfloor$ steps [11, Chapter II]. Choosing Δt_0 small enough also guarantees $\bar z_k \in K$ with $\operatorname{dist}(\bar z_k, \partial K) \ge \rho/2$ for all $k \le \lfloor T/\Delta t\rfloor$ and $\Delta t \le \Delta t_0$.

Part (i). Let $\delta_k = z_k^{(N)} - \bar z_k$ and let $\tau = \min\{k : z_k^{(N)} \notin K\}$. For $k < \tau$ the update gives $\delta_{k+1} = \delta_k + \Delta t\big[F(z_k^{(N)}) - F(\bar z_k)\big] + \zeta_k$, where ζ_k collects the noise terms and satisfies $\mathbb{E}[\zeta_k \mid \mathcal{F}_k] = 0$ and $\mathbb{E}[\|\zeta_k\|^2 \mid \mathcal{F}_k] \le c_K \Delta t/N$ with $c_K := \big(\sigma_0^2 + (\sigma_P^0)^2\big) \sup_K (x^2 + y^2 + P^2)$. Squaring, taking conditional expectations (the cross term with ζ_k vanishes), and using $\|\delta + \Delta t\,\Delta F\|^2 \le (1 + C\Delta t)\,\|\delta\|^2$ with $C = 2L + L^2$ for $\Delta t \le 1$, we obtain

$$\mathbb{E}\big[\big\|\delta_{(k+1)\wedge\tau}\big\|^2\big] \le (1 + C\Delta t)\,\mathbb{E}\big[\|\delta_{k\wedge\tau}\|^2\big] + \frac{c_K \Delta t}{N}.$$

The discrete Grönwall inequality over $k \le \lfloor T/\Delta t\rfloor$ yields $\max_k \mathbb{E}[\|\delta_{k\wedge\tau}\|^2] \le c_K T e^{CT}/N =: C_1(T)/N$, uniformly in $\Delta t \in (0, \Delta t_0]$. On the event $\{\max_k \|\delta_{k\wedge\tau}\| \le \rho/2\}$ the stopped process never exits K, so $\tau > \lfloor T/\Delta t\rfloor$ and the stopped and unstopped deviations coincide; by the union bound and Chebyshev's inequality,

$$\mathbb{P}\Big(\max_{0\le k\le\lfloor T/\Delta t\rfloor} \|\delta_{k\wedge\tau}\| > \epsilon\Big) \le \sum_{k=0}^{\lfloor T/\Delta t\rfloor} \frac{\mathbb{E}[\|\delta_{k\wedge\tau}\|^2]}{\epsilon^2} \le \frac{(T/\Delta t + 1)\,C_1(T)}{N\epsilon^2} \tag{32}$$

for every $\epsilon \in (0, \rho/2]$, which tends to 0 as $N \to \infty$ at fixed Δt. This proves both assertions of part (i).

Part (iii). By the triangle inequality and part (ii), $\max_k \big\|z_k^{(N)} - z(k\Delta t_N)\big\| \le \max_k \|\delta_k\| + C_2(T)\Delta t_N$. Given $\epsilon > 0$, the second term is eventually below $\epsilon/2$, and by (32) with $\epsilon/2$ the first exceeds $\epsilon/2$ with probability at most $O\big(1/(N\Delta t_N \epsilon^2)\big) \to 0$ since $N\Delta t_N \to \infty$. □

Remark 5.2. *The condition $N\Delta t_N \to \infty$ in part (iii) stems from the elementary union bound in (32); it could be weakened by controlling the martingale part of δ_k with Doob's maximal inequality, at the cost of heavier notation. We do not pursue this refinement here.*

Remark 5.3. *Theorem 5.1 establishes that the predator–prey ODE is the joint large-N, small-Δt limit of the stochastic market model. For $N < \infty$, stochastic fluctuations of order $O(1/\sqrt{N})$ generate the fat-tailed returns and volatility clustering documented in Section 5.4 below, without any exogenous news shocks; in the joint limit these finite-size effects vanish and the smooth deterministic oscillations of the ODE are recovered.*

Remark 5.4 (Scope: the herding case $\kappa > 0$)**.** *Theorem 5.1 is stated for $\kappa = 0$ and* does not apply *when $\kappa > 0$: the buyer growth rate $r_B(t)$ in (29) then depends on the lagged price ratio P_t/P_{t-1}, the process is no longer Markovian in*

(B_t, S_t, P_t), *and density-dependent convergence arguments in the spirit of Kurtz [16] do not apply directly. We therefore leave the mean-field limit of the* $\kappa > 0$ *system as an open problem; we expect it to require McKean–Vlasov techniques for non-Markovian, path-dependent interactions. The finite-*N *herding case is explored only as* exploratory numerics*: in the simulation of Figure 5 (*$N = 1000$*,* $\kappa = 0.4$*) the trend-following feedback produces a leptokurtic log-return distribution and pronounced volatility clustering, neither of which is present in the* $\kappa = 0$ *joint limit.*

Figure 5 presents the finite-N stochastic market dynamics (with herding, $\kappa > 0$) for the parameter set

$$(r_B^0, m_S, a_{BS}, b_{BS}, \sigma_0, \sigma_P^0, \eta, \kappa) = (0.05, 0.05, 3\times10^{-4}, 3\times10^{-4}, 0.04, 0.05, 0.1, 0.4),$$

with $N = 1000$ and $\Delta t = 1$ over $T = 500$ periods; via (27) these values correspond to $\alpha_{BS} = \beta_{BS} = 0.3$.

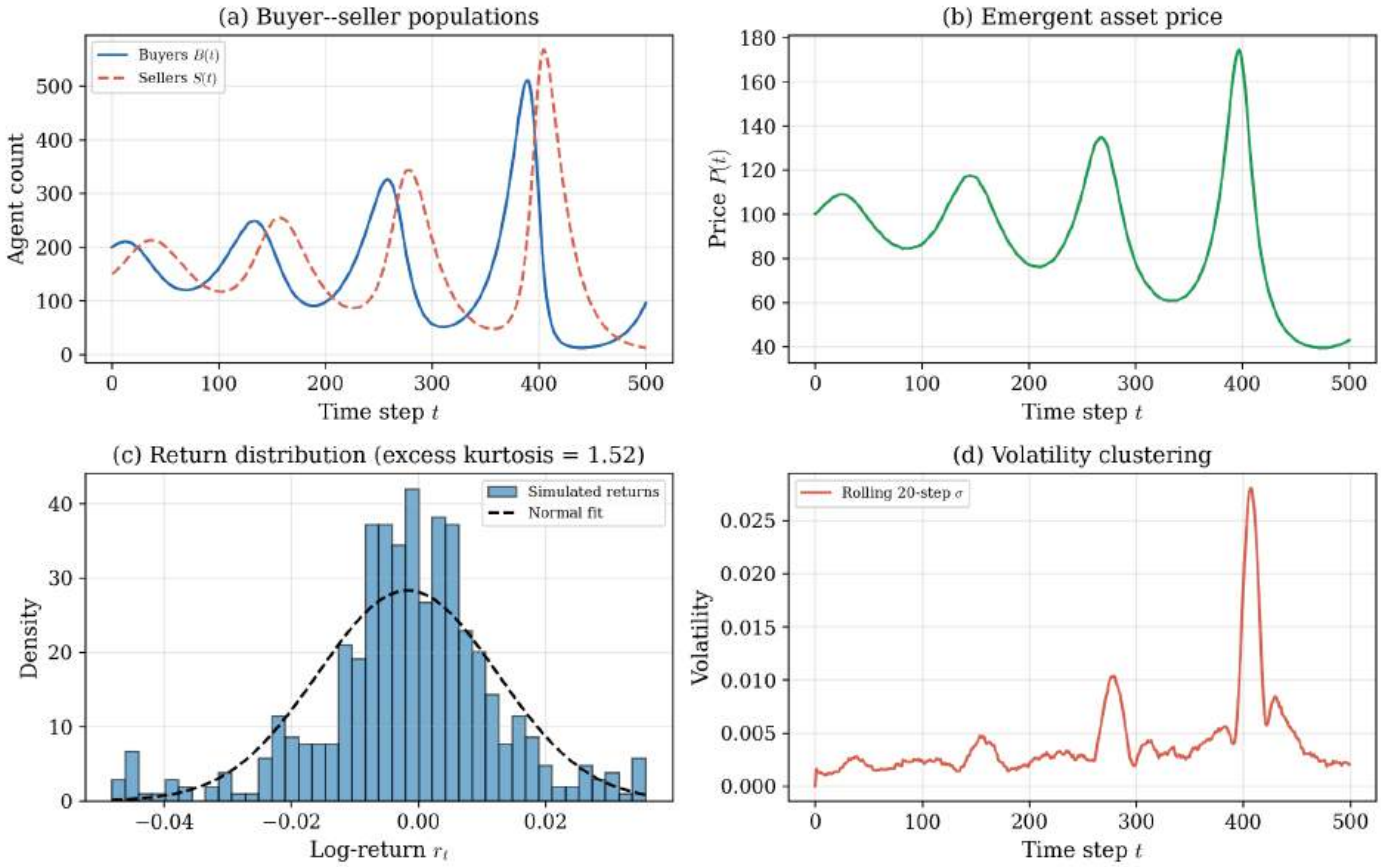


Figure 5. Stochastic simulation of the market model (28) over $T = 500$ periods with $N = 1000$, $\Delta t = 1$, and parameter values $(r_B^0, m_S, a_{BS}, b_{BS}, \sigma_0, \sigma_P^0, \eta, \kappa) = (0.05, 0.05, 3\times10^{-4}, 3\times10^{-4}, 0.04, 0.05, 0.1, 0.4)$ (seed 42). **(a)** Buyer (blue) and seller (red, dashed) aggregates exhibit bounded, anti-correlated oscillations around the deterministic predator–prey cycle. **(b)** Emergent asset price $P(t)$ oscillates with the order imbalance. **(c)** The log-return distribution is leptokurtic (excess kurtosis 1.52 for this seed), departing from the Gaussian fit. **(d)** The rolling volatility exhibits clustering. Because $\kappa = 0.4 > 0$, Theorem 5.1 does *not* apply to this simulation: panels (a)–(d) are exploratory numerics for the herding regime, whose mean-field limit remains open (Remark 5.4). For $\kappa = 0$, Theorem 5.1 guarantees that such finite-size effects vanish in the joint limit $N \to \infty$, $\Delta t \to 0$.

5.3 Numerical Implementation, Reproducibility, and Sensitivity

All simulations were carried out in Python 3.11 with NumPy, SciPy, and Matplotlib; the Jupyter notebook reproducing every figure is provided as supplementary material. Deterministic systems (Figures 1, 2, 3(a)-(b), and 4) were integrated with `scipy.integrate.solve_ivp` (explicit Runge–Kutta RK45; `max_step` $= 0.02$ for Figure 1, and `rtol` $= 10^{-10}$, `atol` $= 10^{-12}$ for the others). The stochastic debt–capital system (18) in Figure 3(c) was simulated by Euler–Maruyama with $\Delta t = 0.05$ and 4000 Monte-Carlo paths (NumPy `default_rng`, seed 0); the market model (28) in Figure 5 uses $\Delta t = 1$, $N = 1000$, and seed 42. All figures are rendered at 300 dpi.

Regarding sensitivity, the qualitative conclusions drawn from Figures 1–3 are not parameter-tuned–the center structure, the first integrals, and the drift rate $\frac{1}{2}(\sigma_C^2 r_D + \sigma_D^2 r_C)$ are theorems valid for *all* positive parameter values (Propositions 2.2 and 3.2, Theorem 4.4), so only quantitative features such as period and amplitude vary with the parameters. The long-run outcome in Figure 4 is likewise characterized exactly, for every parameter choice, by the sign of the closed-form exponent

(26) together with the unconditional instability of E^{**} (Theorem 4.8); the displayed extinction regime corresponds to $\lambda_D < 0$, and $\lambda_D > 0$ would instead produce re-invasion of debt. For the stochastic simulation of Figure 5, whose fine structure is seed-dependent, we re-ran the experiment for seeds 0–9: the excess kurtosis of log-returns ranged over [1.38, 2.03] (positive in every run) and volatility clustering was present in all runs, so the qualitative conclusions of panels (c)–(d) are robust to the realization of the noise.

5.4 Predecessor-Model Evidence

The *predecessor* models on which our framework builds have independent empirical support, summarized below. We stress that these studies validate the established models (Goodwin, Crookes–Blignaut, Montero, Keen), not the specific new claims of this paper; direct empirical tests of Theorems 4.4, 4.8, and 5.1 are left for future work.

1. *Goodwin cycles in OECD economies.* Harvie [12] estimated the Goodwin model (8) for ten OECD countries, documenting quantitative agreement between the model's predictions and the observed counter-cyclical relationship between the wage share and the employment rate, with structurally stable parameters across countries.

2. *Steel industry trophic cascades.* Crookes and Blignaut [5] calibrated system (13) to South African industry production indices for 1970–2010, reporting goodness-of-fit $R^2 > 0.85$ for the cyclical component.

3. *Equity return distributions.* Montero [22] demonstrated that the stochastically perturbed buyer–seller system (14) produces return distributions with excess kurtosis in the range $[3, 7]$, consistent with the empirically documented fat tails of daily returns on major equity indices.

4. *Pre-crisis US debt dynamics.* Keen [15] calibrated a Minskyan debt–capital model to US data for 1945–2007, showing that the ratio of private debt to GDP exhibits growing excursions in the decade preceding the 2008 financial crisis, qualitatively consistent with the noise-induced outward energy drift of Theorem 4.4(iv).

5.5 Comparative Summary of Model Properties

Table 3 provides a unified comparison of the five main model classes analyzed in this paper, listing the predator–prey species, the equilibrium type, and the key novel result associated with each.

Table 3. Comparative properties of the predator–prey models developed in this paper. Novel results established herein are indicated in boldface.

Model	Prey	Predator	Equilibrium type	Key result
Basic LV (1)	x	y	Nonlinear center	First integral; Props. 2.2–2.5
Goodwin (8)	Employment v	Wage share ω	Nonlinear center	LV isomorphism; Prop. 3.2
Debt–Capital (16)	Capital C	Debt D	Center / noise drift	**Minsky formulation; Thm. 4.4**
Super-predator (20)	C, D	$\mathcal{S}$	Unstable interior; boundary cycles	**Instability & extinction exponent; Thm. 4.8**
Stoch. market model (28)	Buyers B	Sellers S	Noisy LV cycles	**Mean-field & continuum limit; Thm. 5.1**

6 Policy Implications

The predator–prey framework developed in this paper suggests a set of qualitatively grounded policy readings. Each is obtained by identifying the structural parameter that, when perturbed, changes the amplitude of cyclical fluctuations, the equilibrium leverage, or—for the three-species system—the fate of the debt market, according to the results established in Theorems 4.4–5.1. An important caveat applies throughout this section: statements linking real-world policy instruments to model parameters are *interpretive mappings within the model*, not quantitative results established by the analysis; we therefore use conditional wording ("may be interpreted as", "could be represented as") deliberately.

Wage policy and automatic stabilizers. In the Goodwin model (8), the amplitude of business cycles is proportional to the distance of the orbit from the center E^* given in (11). Raising the unemployment insurance replacement rate may be interpreted, within the model, as reducing the Phillips-curve slope ρ (i.e., wage sensitivity to employment), which by

Proposition 3.2 compresses the orbit in the (ω, v)-plane and moderates cycle amplitude. A statutory minimum-wage floor could be represented as a lower bound on ω, preventing wage-share trajectories from entering the deflationary region $\omega \ll \omega^*$ [12].

Macroprudential regulation and noise-induced fragility. By Theorem 4.4(iv), the conserved energy of the stochastic debt–capital system drifts strictly outward at the rate $\frac{1}{2}(\sigma_C^2 r_D + \sigma_D^2 r_C) > 0$ under *any* noise; there is no deterministic stable regime to be "restored" by an r_D-versus-r_C inequality. Macroprudential policy nonetheless has two natural readings within the model. First, measures that suppress debt-side volatility—loan-to-value limits, countercyclical capital buffers, debt-service coverage requirements—could be represented as reducing σ_D, and hence the term $\sigma_D^2 r_C$ in the drift, slowing the outward energy migration in expectation. Second, by Theorem 4.4(iii) the equilibrium leverage ratio $D^*/C^* = b_{DC} r_C/(a_{DC} r_D)$ is increasing in r_C and decreasing in r_D and is lowered by increasing a_{DC} (which stricter debt-service requirements may be read as doing); shifting this ratio governs how the unavoidable noise-driven excursions are distributed between the debt and capital coordinates. Keen [15] proposes a *debt jubilee*—a one-time reduction in D—as a discrete intervention returning a high-leverage trajectory to a lower sublevel set of H, i.e., closer to E^*.

Regulating financial super-predators. Theorem 4.8 changes the nature of the policy question for the three-species system: because the interior equilibrium is unstable for *all* positive parameters, no adjustment of extraction or origination coefficients can stabilize interior coexistence. Within the model, policy instead operates on *which boundary regime prevails*, through the extinction exponent (26), whose comparative statics are $\partial\lambda_D/\partial c_{DS} = -r_C/e_{CS} < 0$, $\partial\lambda_D/\partial g_{CS} = +b_{DC} r_{\mathcal{S}}/g_{CS}^2 > 0$, and $\partial\lambda_D/\partial r_{\mathcal{S}} = -b_{DC}/g_{CS} < 0$. Within the interpretation of the model, restrictions on credit-default instruments and securitization spreads could be represented as reducing c_{DS}, which raises λ_D and favours the survival of ordinary credit relative to the intermediated boundary regime; Tobin-type transaction taxes could be represented as reducing the profitability of intermediation (lower f_{DC}, higher effective $r_{\mathcal{S}}$), mechanisms discussed qualitatively by Stiglitz [29] and Goldstein [9]. We stress that these are interpretive mappings; the model itself establishes only the dependence of λ_D and E^{**} on the structural parameters.

Market transparency and information policy. By Theorem 5.1, the stochastic market model converges to the deterministic dynamics in the joint limit $N \to \infty$, $\Delta t \to 0$. Policies that deepen markets—mandatory pre-trade transparency, central clearing, a consolidated tape—may be interpreted, within the model, as increasing the effective size N, which reduces the $O(1/\sqrt{N})$ fluctuations and improves the approximation of the stochastic system by the deterministic predator–prey dynamics, in which bubble and crash dynamics are absent. Similarly, circuit breakers or short-selling restrictions could be represented as reducing the trend-following coefficient κ in (29), limiting the positive-feedback amplification that generates fat-tailed returns in the finite-N system; we note that the $\kappa > 0$ regime lies outside the scope of Theorem 5.1 (Remark 5.4).

7 Conclusion and Future Research

This paper has developed a rigorous, unified mathematical framework for applying predator–prey dynamical systems to economic and financial phenomena. The main analytical results are as follows.

Starting from the classical Lotka–Volterra equations, we established positive invariance and global existence of solutions (Proposition 2.1), proved the existence of a conserved Hamiltonian via explicit computation (Proposition 2.2), and derived the period formula for small-amplitude oscillations (Corollary 2.3). For the Rosenzweig–MacArthur logistic extension, we identified the precise carrying-capacity threshold $K_c = 2x^* + 1/(ah)$ with $x^* = m/(b - mah)$, at which a Hopf bifurcation occurs and limit cycles emerge (Proposition 2.5).

In the economic domain, we proved that the Goodwin growth-cycle model is an exact algebraic isomorphism of the Lotka–Volterra system (Proposition 3.2), thereby transferring all conservation and periodicity results to the macroeconomic setting.

In the financial domain, we derived a two-species debt–capital predator–prey model from microeconomic first principles (Assumption 4.2), constructed an explicit first integral / Lyapunov function, and gave a rigorous Lyapunov-based formulation of Minsky's hypothesis: the deterministic system is a neutral center for all positive parameters, while under Itô noise the expected energy drifts strictly outward at the rate $\frac{1}{2}(\sigma_C^2 r_D + \sigma_D^2 r_C)$ (Theorem 4.4), so that no deterministic r_D-versus-r_C threshold governs stability. This complements Asada's [2] predator–prey treatment of Minsky's hypothesis. We then introduced and analyzed a three-species super-predator system: under an explicit parameter condition a unique interior equilibrium exists (Proposition 4.7), but it is unstable for *all* positive parameter values, so stable interior coexistence is impossible; on the $D = 0$ boundary face the dynamics reduce to a classical Lotka–Volterra pair, and the closed-form transversal exponent λ_D of (26) decides, uniformly across all boundary cycles, whether debt is driven to extinction (Theorem 4.8), in quantitative agreement with the simulations.

Finally, we formulated a finite-size stochastic market generalization of the buyer–seller model with herding, with explicit density-dependent scaling, and proved a two-step limit theorem (Theorem 5.1): at fixed time step the size-N

process converges in probability to the deterministic Euler map, and in the joint limit $N \to \infty$, $\Delta t \to 0$ it converges in probability, uniformly on compact time intervals, to the deterministic Lotka–Volterra ODE.

The results of this paper open several mathematically rich avenues for future investigation.

Behavioral and heterogeneous-agent extensions

Incorporating prospect theory [14] and salience-weighted attention into the buyer–seller market model (28) would yield a model in which the effective predation rate a_{BS} depends on the recent history of losses and gains. A rigorous mean-field analysis analogous to Theorem 5.1 in this non-Markovian setting would require new techniques from the theory of McKean–Vlasov equations.

Network-embedded predator–prey models

Real economies are networks: firms, banks, and households are connected through credit, supply-chain, and ownership relationships. Embedding the dynamics of (20) on a random graph [13] would reveal how network topology (degree distribution, clustering, assortativity) shapes the amplitude and propagation speed of financial instability, and would raise new questions about how network structure reshapes the extinction exponent λ_D of Theorem 4.8.

Stabilized variants, bifurcation, and chaos analysis.

Theorem 4.8 rules out Hopf bifurcations of the interior equilibrium for (20) itself (Remark 4.10). Damped variants—for example, logistic self-limitation of capital—restore the possibility of stable coexistence and Hopf bifurcations, and are the natural setting in which to investigate period-doubling routes to complex dynamics with dedicated numerical bifurcation software (e.g., AUTO-07P, MATCONT) and computer-assisted proof techniques.

Bayesian structural estimation.

Bayesian estimation of the Goodwin model (8) and the debt–capital model (16) via particle-filter methods applied to high-frequency national-accounts and credit data would sharpen the quantitative content of the framework, produce posterior distributions over the equilibrium leverage ratio D^*/C^* and the extinction exponent λ_D, and enable formal hypothesis testing against competing macro-finance models.

Ecological–economic coupling and sustainability.

Predator–prey models are structurally suited to coupling economic growth with biophysical limits [26]. Introducing a natural-capital "prey" variable—depleted by economic "predation" via resource extraction or carbon emissions—into the Goodwin framework would yield a mathematically tractable, empirically calibratable model for planetary-boundary sustainability analysis.

Partial differential equation extensions.

The reaction–diffusion system (6) raises natural questions about the existence of traveling-wave solutions connecting spatially homogeneous steady states, the Turing instability mechanism in the context of economic geography, and the well-posedness of the associated boundary-value problems in weighted Sobolev spaces.

In summary, the predator–prey paradigm developed in this paper provides a rigorous, parsimonious, and empirically tractable mathematical framework for analyzing the cyclical, fragile, and self-referential dynamics of modern financial capitalism. The integration of this framework with machine learning, high-frequency microstructure data, and network-theoretic tools represents a promising agenda for both mathematical research and policy analysis.

Conflicts of Interest

The authors declare no conflicts of interest.

Author Contributions

We describe contributions following the CRediT taxonomy. **Deepak Bastola:** Conceptualization, Methodology, Formal analysis, Writing – original draft. **Pitambar Acharya:** Conceptualization, Methodology, Formal analysis, Writing – original draft. *(Pitambar Acharya and Deepak Bastola contributed equally and are joint first authors.)* **Dipak Dulal:** Writing – review & editing. **Pawan Kumar BK:** Writing – review & editing. All authors read and approved the final manuscript.

Funding

This research received no external funding.

Code Availability Statement

The code used in this study is publicly available on GitHub at: https://github.com/deepakbastola/PredatorPrey.

Institutional Review Board Statement

Not applicable. This study did not involve human participants or animals.

Informed Consent Statement

Not applicable.

Generative AI Disclosure

Generative AI was used as a language support tool during the preparation of this manuscript. Its use was limited to improving clarity, refining wording, correcting grammatical errors, and enhancing overall readability. All AI-assisted suggestions were independently reviewed, revised where appropriate, and approved by the authors, who retain full responsibility for the accuracy, originality, and integrity of the final manuscript.

References

[1] L. M. Addison, B. S. Bhatt, and D. R. Owen. A prey–predator model for investing in stocks. *International Journal of Pure and Applied Mathematics*, 107(2):487–502, 2016.

[2] T. Asada. Modeling financial instability. *European Journal of Economics and Economic Policies: Intervention*, 9(2): 215–232, 2012.

[3] R. Axtell. Why agents? On the varied motivation for agent-based modeling in the social sciences. *Journal of Artificial Societies and Social Simulation*, 11(4), 2008. Article 9.

[4] C. Chiarella, G. Iori, and J. Perelló. The impact of heterogeneous trading rules on the limit order book and order flows. *Journal of Economic Dynamics and Control*, 33(3):525–537, 2009.

[5] D. Crookes and J. Blignaut. Predator–prey analysis using system dynamics: an application to the steel industry. *South African Journal of Economic and Management Sciences*, 19(5):733–748, 2016.

[6] M. Desai, B. Henry, A. Mosley, and M. Pemberton. A clarification of the Goodwin model of the growth cycle. *Journal of Economic Dynamics and Control*, 30(12):2661–2670, 2006.

[7] J. M. Epstein and R. Axtell. *Growing Artificial Societies: Social Science from the Bottom Up*. Brookings Institution Press, Washington, D.C., 1996.

[8] L. Gardini, R. Lupini, and M. G. Messia. Hopf bifurcation and transition to chaos in the Lotka–Volterra equation. *Journal of Mathematical Biology*, 27(3):259–272, 1989.

[9] J. Goldstein. A three-class predator–prey model with financial super-predators: The financial profit squeeze. Technical Report Working Paper No. 515, Political Economy Research Institute, University of Massachusetts Amherst, 2020.

[10] R. M. Goodwin. A growth cycle. In C. H. Feinstein, editor, *Socialism, Capitalism and Economic Growth*, pages 54–58. Cambridge University Press, Cambridge, 1967.

[11] P. Hartman. *Ordinary Differential Equations*. SIAM, Philadelphia, 2nd edition, 2002.

[12] D. Harvie. Testing Goodwin: growth cycles in ten OECD countries. *Cambridge Journal of Economics*, 24(3):349–376, 2000.

[13] M. O. Jackson and B. W. Rogers. Meeting strangers and friends of friends: how random are social networks? *American Economic Review*, 97(3):890–915, 2007.

[14] D. Kahneman and A. Tversky. Prospect theory: an analysis of decision under risk. *Econometrica*, 47(2):263–291, 1979.

[15] S. Keen. *Debunking Economics: The Naked Emperor Dethroned?* Zed Books, London, 2nd edition, 2011.

[16] T. G. Kurtz. Solutions of ordinary differential equations as limits of pure jump Markov processes. *Journal of Applied Probability*, 7(1):49–58, 1970.

[17] Y. A. Kuznetsov. *Elements of Applied Bifurcation Theory*. Springer, New York, 3rd edition, 2004.

[18] A. J. Lotka. Analytical note on certain rhythmic relations in organic systems. *Proceedings of the National Academy of Sciences*, 6(7):410–415, 1920.

[19] T. Lux and M. Marchesi. Scaling and criticality in a stochastic multi-agent model of a financial market. *Nature*, 397 (6719):498–500, 1999.

[20] X. Mao, G. Marion, and E. Renshaw. Environmental Brownian noise suppresses explosions in population dynamics. *Stochastic Processes and their Applications*, 97(1):95–110, 2002.

[21] H. P. Minsky. *Stabilizing an Unstable Economy*. Yale University Press, New Haven, 1986.

[22] M. Montero. Predator–prey model for stock market fluctuations, 2008. Preprint, arXiv:0810.4844.

[23] J. D. Murray. *Mathematical Biology I: An Introduction*. Springer, New York, 3rd edition, 2002.

[24] J. D. Murray. *Mathematical Biology II: Spatial Models and Biomedical Applications*. Springer, New York, 3rd edition, 2003.

[25] D. H. Nguyen and G. Yin. Coexistence and exclusion of stochastic competitive Lotka–Volterra models. *Journal of Differential Equations*, 262(3):1192–1225, 2017.

[26] E. Ostrom. A general framework for analyzing sustainability of social-ecological systems. *Science*, 325(5939):419–422, 2009.

[27] M. L. Rosenzweig. Paradox of enrichment: destabilization of exploitation ecosystems in ecological time. *Science*, 171 (3969):385–387, 1971.

[28] L. Shaikhet and A. Korobeinikov. Persistence and stochastic extinction in a Lotka–Volterra predator–prey stochastically perturbed model. *Mathematics*, 12(10):1588, 2024.

[29] J. E. Stiglitz. *Freefall: America, Free Markets, and the Sinking of the World Economy*. W. W. Norton & Company, New York, 2010.

[30] V. Volterra. Fluctuations in the abundance of a species considered mathematically. *Nature*, 118(2972):558–560, 1926.

[31] M. L. Zeeman. Hopf bifurcations in competitive three-dimensional Lotka–Volterra systems. *Dynamics and Stability of Systems*, 8(3):189–217, 1993.

Publisher's Note. Statements, opinions, and data contained in publications are solely those of the individual author(s) and contributor(s). The publisher and editors disclaim responsibility for injury to people or property resulting from ideas, methods, instructions, or products referred to in the content.